

## Specific Heat Capacity Determination by DSC

April 19, 10:00am - 11:00am EDT

Specific heat capacity ( $c_p$ ) is an important, temperature-dependent material property and is often specified in material data sheets. It is a key property for improving technical processes such as injection molding, spray drying, or crystallization, as well as for the safety analysis of chemical processes and the design of chemical reactors.

Watch this session during the WAS Virtual Conference:



Dr. Jürgen Schawe

[Register Now](#)

# Micro-Optics 3D Printed via Multi-Photon Laser Lithography

Diana Gonzalez-Hernandez, Simonas Varapnickas, Andrea Bertoncini, Carlo Liberale,\* and Mangirdas Malinauskas\*

The field of 3D micro-optics is rapidly expanding, and essential advances in femtosecond laser direct-write 3D multi-photon lithography (MPL, also known as two-photon or multi-photon polymerization) are being made. Micro-optics realized via MPL emerged a decade ago and the field has exploded during the last five years. Impressive findings have revealed its potential for beam shaping, advanced imaging, optical sensing, integrated photonic circuits, and much more. This is supported by a game-changing and increasing industrial interest from key established companies in this field. In this review, the origin and the advancement of micro-optics fabrication with MPL are detailed by describing the chronology, distinguishing discrete application groups, providing generalized technical data on the processes and available materials, and discussing the foreseen near-future advances.

## 1. Introduction

The rapid growth of laser applications has stimulated the demand and supply for new optical components. At the same time, devices are becoming miniaturized and highly integrated to maximize functionality. Here, the field of laser technology and industrial trends meet to create synergy.

While the first use of ultrafast lasers for 3D structuring was proposed in 1991 for optical data storage,<sup>[1]</sup> their use to create

3D printed objects was first presented by Maruo in a technology-opening article in 1997,<sup>[2]</sup> where the use of this technology to fabricate micro-optics was also envisaged. The serial writing method of this technique offered flexibility for free-form fabrication, but was limited by its throughput.<sup>[3]</sup> It took some years for the technology to mature from proof-of-principle level to additive manufacturing as a tool for efficient and reliable fabrication in the modern lab.<sup>[4–6]</sup> Though the first micro-optical elements were demonstrated as early as 2006,<sup>[7]</sup> the major efforts and results only started to emerge in 2010,<sup>[8,9]</sup> together with the development of hybrid organic–inorganic materials,<sup>[10,11]</sup> and rapidly


accelerated with the implementation of commercial 3D lithography systems.<sup>[12–14]</sup> By 2020, ultrafast laser 3D printing, also known as two-photon polymerization (TPP or 2PP), multi-photon lithography (MPL),<sup>[15–17]</sup> or simply laser direct writing (LDW), also in literature referenced as direct laser writing (DLW),<sup>[18]</sup> was already an established technique for routine fabrication of diverse micro-optical single elements, stacked components, and integrated devices.<sup>[19–21]</sup> The latest advances in the 3D printing of free-form micro-optics are enhanced by optical grade materials of high refractive index ( $n$ ) polymers,<sup>[22]</sup> high-performance hybrids,<sup>[23]</sup> and optically active<sup>[24]</sup> or pure inorganic glasses.<sup>[25]</sup> **Figure 1** shows the development of the technique in terms of published papers and citations, defining an “innovator stage” of the technology followed from 2015 by the “early adopters stage.” Examples of micro-optical elements fabricated using MPL and the growth in the complexity of the structures that can be achieved by this technique are also shown in **Figure 1**.

The advances in this scientific field attracted the attention of the related laser-assisted precision additive manufacturing industry. First, in 2007 Nanoscribe GmbH and in 2008 Workshop of Photonics established companies oriented toward commercialization of this technology aimed at general wide angle application fields. While in 2013, Multiphoton Optics GmbH and Femtika UAB were established and made micro-optics a significant part of their targeted applications. Finally, in 2017, Vanguard Photonics GmbH manufactured dedicated MPL equipment for micro-lenses and wire bond production. Other companies targeting more diverse applications have continued to emerge, such as UpNano established in 2018, and focusing mostly on biomedical applications yet also offering solutions

D. Gonzalez-Hernandez, A. Bertoncini, C. Liberale  
Biological and Environmental Science and Engineering Division  
King Abdullah University of Science and Technology (KAUST)  
Thuwal 23955-6900, Saudi Arabia  
E-mail: carlo.liberale@kaust.edu.sa

S. Varapnickas, M. Malinauskas  
Laser Research Center  
Physics Faculty  
Vilnius University  
Vilnius LT-10223, Lithuania  
E-mail: mangirdas.malinauskas@ff.vu.lt

C. Liberale  
Computer, Electrical and Mathematical Sciences and Engineering  
King Abdullah University of Science and Technology (KAUST)  
Thuwal 23955-6900, Saudi Arabia

 The ORCID identification number(s) for the author(s) of this article can be found under <https://doi.org/10.1002/adom.202201701>.

© 2022 The Authors. Advanced Optical Materials published by Wiley-VCH GmbH. This is an open access article under the terms of the Creative Commons Attribution License, which permits use, distribution and reproduction in any medium, provided the original work is properly cited.

DOI: 10.1002/adom.202201701

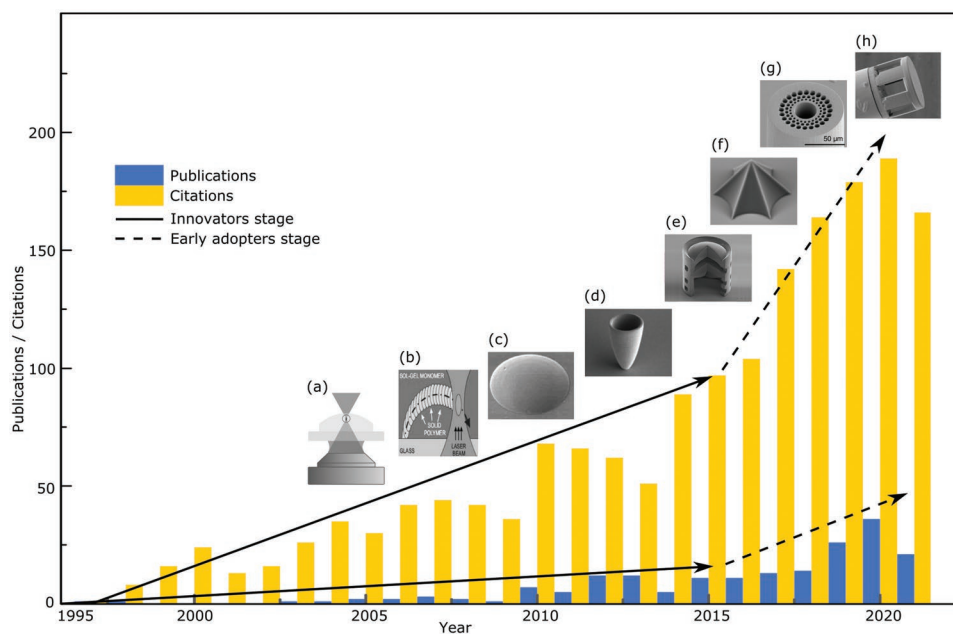


**Figure 1.** The dynamics of original papers published and citations over the last 25 years. The number of original papers corresponds to the references included in the literature list of the review. The number of citations stands for the data retrieved from the Web of Science search for keywords “micro-optics” + “laser lithography.” a) Schematic of an MPL system. b) Different fabrication strategies emerged, such as the implementation of UV lithography. Single elements as c) spherical lenses fabricated as building-blocks for micro-optics, and d) post-processing techniques such as metallization applied for particular functionalization of the micro-elements. MPL allowed fabrication on different substrates including glass cover slits and optical fibers of e) stacked micro-lenses, and complex 3D structures such as f) wrinkled axicons, g) photonic crystal fiber-like structures, and h) a micro-lens array for a hyper-telescope. b) Adapted with permission.<sup>[9]</sup> Copyright 2010, IOP Publishing. c) Adapted with permission.<sup>[26]</sup> Copyright 2010, American Institute of Physics. d) Adapted with permission.<sup>[27]</sup> Copyright 2011, American Institute of Physics. e) Adapted with permission.<sup>[28]</sup> Copyright 2017, Elsevier Ltd. f) Adapted with permission.<sup>[29]</sup> Copyright 2016, The Optical Society. g) Adapted with permission.<sup>[30]</sup> Copyright 2020, The Optical Society. h) Adapted with permission.<sup>[31]</sup> Copyright 2021, The Optical Society.

for production of micro-optics related components and materials. There are also now a number of MPL commercial setups specifically for micro-optics, for example, Quantum X Align (by NanoScribe).

Within the scope of this topical review, we will provide an overview of the chronology and development of the field, featuring the most prominent advances, and grouping the achievements by their operating principles or applications. A few milestones showcasing the progress and advances in the complexity of optical micro-structures created with MPL are shown in chronological sequence in Figure 1 and will be described in more detail in the following sections. The tendency was that efforts were focused toward developing technology and proving its feasibility for miniaturizing prototype micro-optics. Later, this was followed by the coupling of several functionalities, which was in principle possible only due to dense integration of individual modalities. Finally, optical grade materials started to be exploited for heavy duty applications in parallel to assemble into established platforms (micro-chips). Further advances are expected in establishing advanced metrology dedicated for 3D micro-optics specifically, followed by standardization of the protocols for comparison and repeatability. All of the aforementioned is covered sequentially in the following sections: 1. Introduction; 2. Principles and developments of ultrafast laser 3D micro-/nanolithography; 3. Fabrication modalities; 4. Single micro-optical elements; 5. Applications; 6. Materials and post-processing; 7. Summary and conclusions.

## 2. Principles and Developments of Ultrafast Laser 3D Micro-/Nanolithography

The principle workflow of MPL is already well established and currently predominantly operated as a standard procedure.<sup>[4–6,15,32]</sup> Although there are still active debates regarding the photo-physical/chemical initiation mechanisms in spatiotemporally confined light conditions,<sup>[17]</sup> ultrashort pulsed lasers are currently dominant,<sup>[33]</sup> while longer pulse duration (ps, ns)<sup>[34,35]</sup> or even CW<sup>[36]</sup> operating light sources are also suitable for this purpose. The details of the photoexcitation mechanisms are not covered in this review, but for simplicity, we accept it as a nonlinear light–matter interaction (whether the nonlinearity is caused by thresholded excitation or material response behavior). The typical setups employ 100–300 fs pulses of 100 kHz–80 MHz repetition rates delivering approximately  $10^{12}$  W cm<sup>-2</sup> intensities at the focus. The used radiation should not interact significantly in a linear manner; thus, it is chosen to be of VIS (centered at 515–532 nm) or more commonly NIR (centered 780–800 nm) wavelengths. Some unconventional parameters like CW, 1 kHz, or 400 nm can also be used for true 3D structuring inducing a localized thermal effect,<sup>[37]</sup> distinct avalanche ionization,<sup>[38]</sup> confined linear absorption,<sup>[39]</sup> or trigger a two-step absorption mechanism.<sup>[40]</sup> Diverse approaches enable specific benefits, such as avoidance of the photo-initiator or reduction of equipment costs and complexity. However, these approaches are still not commonly used for the production of

micro-optical components via LDW technology. Finally, the fact that ultrafast lasers are the dominant technology is reflected by the commercialized laser setups which, almost all, exclusively use femtosecond high pulse repetition rate laser oscillators (Nanoscribe, Workshop of Photonics) or whole amplified systems (Femtika, MultiPhoton Optics).

The principle fabrication MPL sequence is graphically depicted in **Figure 2**. The photo-exposure strategy can be realized in the following ways: 1) serial writing (point-by-point) in a raster or vectorial mode;<sup>[41–43]</sup> 2) interference/holography;<sup>[44–46]</sup> 3) parallel writing;<sup>[47–50]</sup> or 4) continuous volumetric printing.<sup>[51,52]</sup> All of these have certain specific advantages in terms of flexibility for the realization of complex shapes, speeding up production, or allowing working with different resins. Although various methods can be employed to create micro-optical elements, in addition to the resolution (accuracy of the 3D printed objects), their exposure dose and homogeneity, surface quality, and stitching artifacts may influence the efficient refractive index and optical performance. There is no single best method for the production of the whole spectrum of micro-optical geometries as there are no sophisticated and versatile characterization standards established so far. However, original improvements from the scientific community and specific solutions from industry are emerging to satisfy the application-driven demand.

The photo-excitation beam is commonly focused using dry,<sup>[21]</sup> immersion oil,<sup>[9]</sup> or dip-in<sup>[53]</sup> approaches via microscope objectives. Their numerical apertures (NA) and magnifications can be

chosen depending on the required precision (which is inversely proportional to throughput), material used (liquid or sol-gel/solid), and geometry (2.5D or complex free-form 3D) or platform (e.g., glass, silicon or metal substrates, fiber facets, CMOS chips, wire bonding, or hollow micro-fluidic cavities). After exposure, a wet lithography development is carried out where most organic solvents such as alcohols isopropanol, acetone, ethanol, or more aggressive chemicals like 4-methyl-2-pentanone, 1-methoxy-2-propyl acetate, tetrahydrofuran, and toluene can be applied. The exact developer or their mixture depends on the resin and intended etching rate. Additional rinsing in solvent and critical point drying can be employed for cleaner removal of the unexposed matter and retrieving the structures without distortions due to shrinkage and capillary forces. Some post-processing solutions like metal sputtering or atomic layer deposition can be further exploited to increase the functionalities of the micro-optical components. The produced templates can serve as master stamps or be used to make replica molding masks for a well-established nano-imprint and soft-lithography multiplication of nano-/microstructures routes. Recently, heat treatment at elevated temperatures, known as pyrolysis or calcination, was validated to sinter the microstructures by converting them into completely inorganic compounds.

Several parameters influence the resulting characteristics of the micro-optical elements fabricated by MPL. Features are determined depending on the voxel size and the accuracy of the MPL system. The roughness of the structure establishes its surface quality, which impacts its optical performance. Additionally, MPL

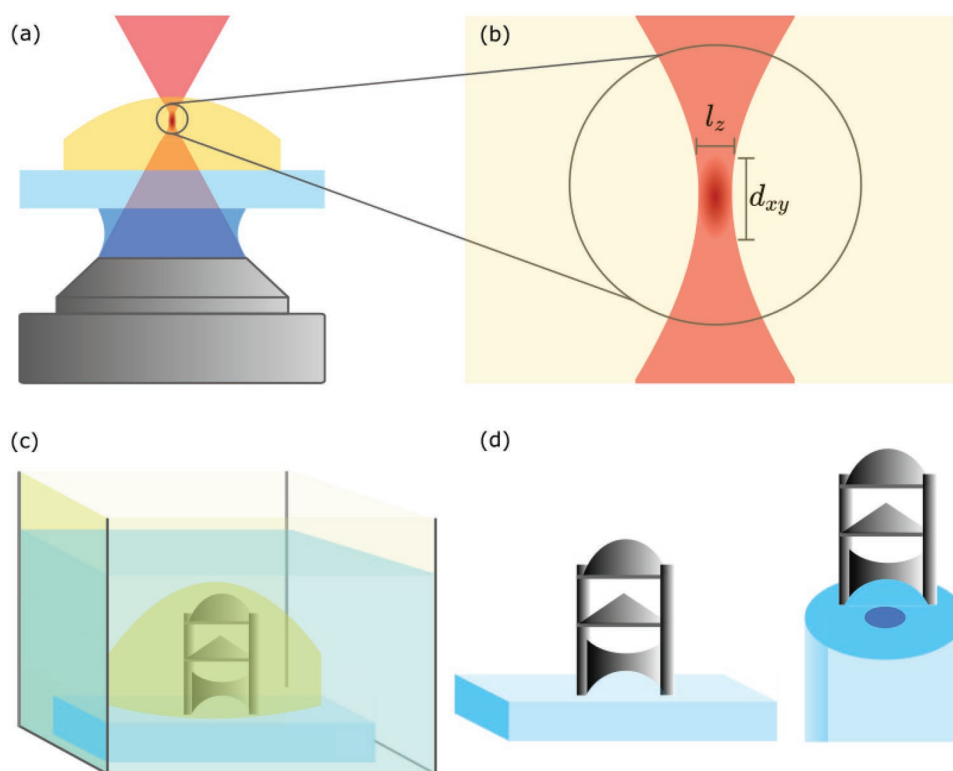


**Figure 2.** Laser direct writing 3D multiphoton nanolithography processes: a) A femtosecond beam is tightly focused into the pre-polymer material confining the light–matter interaction into a (sub-)wavelength scale; b) the beam focus is scanned or the work-piece is translated to materialize the computer model and it is replicated into the corresponding photo-exposed volume; c) a wet chemical development is used to reveal the 3D object; d) a free-form self-standing structure that can be used for a particular optical function or as a template for additional functionalization via post-processing.



**Table 1.** Characteristics of optical structures and MPL technology aspects in the context of micro-optics.

Voxel size	Lateral—from 100 nm <sup>[27]</sup> to 500 nm <sup>[54]</sup> , and axial—from 100 nm <sup>[55]</sup> to 1.5 μm <sup>[54]</sup> , or even higher ones using low NA objectives
Accuracy	Sub-micron ≈100 nm <sup>[56]</sup>
Roughness	From 3 nm <sup>[57]</sup> to order of 100 nm <sup>[13]</sup>
Structure dimensions	Micro-lens diameter—from few μm <sup>[58]</sup> to 2 mm <sup>[57]</sup> Waveguides—core size down to 1 μm and lengths up to 150 μm <sup>[59]</sup>
Throughput (time/lens)	From few minutes <sup>[60]</sup> up to 23 h <sup>[57]</sup> per lens
Parallelization	4 × 4 micro-structure array <sup>[47]</sup>

technology has achieved dimensions from sub-micron to millimeter scale optical structures and fabrication speed down to a few minutes per fabricated structure. **Table 1** presents the different values reported for the principal characteristics of the microstructures and aspects of MPL technology in the context of micro-optics.

### 3. Fabrication Modalities

In MPL fabrication, high control over design, fabrication, and post-fabrication processes allows for ever-expanding possibilities to create unprecedented and high-quality micro-optics. To take advantage of this potential, several fabrication modalities have been developed, where different degrees of freedom are controlled during the fabrication processes, including laser scanning strategy and energy dose per voxel. In this section, we summarize the most important MPL fabrication modalities.

In the basic approach, a single dose per voxel is applied, typically by using constant laser-scanning speed and laser power (corresponding to incident light intensity), leading to a constant voxel size and refractive index across the fabricated structure. Different geometries require specific scanning strategies for the laser spot tracing through the photoresist during fabrication to achieve

smooth surfaces. Generally, the structure's design is sliced into layers and hatched with a specific distance between the parallel lines; this method is favorable for flat surface structures.

Curved profiles are commonly present in micro-optics, and the previously mentioned scanning method creates unwanted steps on the surface, impacting their optical performance. As a solution, the annular scanning mode was proposed as a fabrication method for micro-lenses, providing a better approximation to the curved profiles than the parallel lines, ensuring the lens orbicular symmetry and radial consistency. This method, together with the implementation of continuous variable layer thickness, reduces the defects and improves the surface quality as shown in **Figure 3a**. The height of the layers impacts the surface smoothness, since the 3D structure is manufactured in a layer-by-layer manner. A continuous variable layer thickness was introduced as an optimization of the fabrication of curved surfaces. This method achieved high-quality and smooth-shaped surfaces required in optical elements, such as Fresnel lenses.<sup>[7]</sup>

Another scanning strategy presented is based on spiral paths to polymerize the surface of conical micro-lenses (micro-axicons), controlling the voxel overlap.<sup>[54]</sup>

To overcome the long fabrication time for micro-lenses, Malinauskas (2010)<sup>[9]</sup> presented a different fabrication procedure consisting of a shell-surface polymerization followed by UV curing of the unexposed internal volume after removing the nonfunctional external photoresist as shown in **Figure 3b**. This method combines the high-resolution granted by MPL with a uniform fast UV exposure to create micro-optical components, speeding up the entire fabrication process by a factor of approximately 200.

Nowadays, higher control of fabrication parameters in the MPL process allows the introduction of new degrees of freedom, besides the well-known 3D spatial parameters, permitting different fabrication modalities. Generally, the refractive index and the dispersive properties of the photopolymer material limit the microstructures fabricated by MPL. An additional degree of freedom during fabrication allows control of the refractive index of the photopolymer. A controlled nonconstant fabrication laser intensity enables tuning of the refractive index of the resultant structure up to a 0.3 change

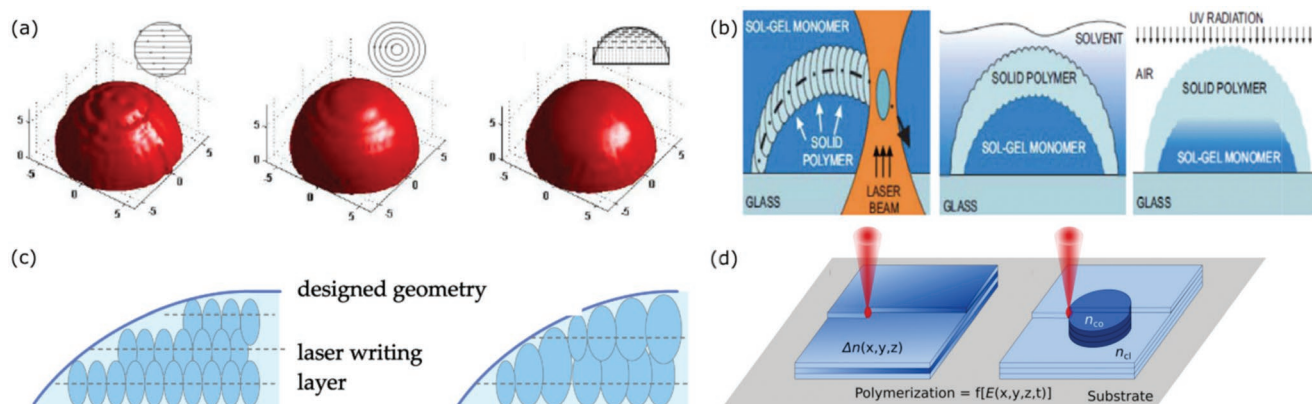


**Figure 3.** a) Parallel linear, annular scanning with fixed layer spacing and, annular scanning with dynamic layer spacing scanning strategies. b) Shell-surface polymerization followed by development, and UV curing of the inner volume. c) Refractive index controlled by dynamically changing the laser power in the fabrication process. d) Comparison of voxel size definition of classic TPL versus 2GL. a) Adapted with permission.<sup>[7]</sup> Copyright 2016, The Optical Society. b) Adapted with permission.<sup>[9]</sup> Copyright 2010, IOP Publishing. c) Adapted with permission.<sup>[62]</sup> Copyright 2021, The Optical Society. d) Adapted with permission.<sup>[60]</sup> Copyright 2021, The Optical Society.

for visible light. This method has been demonstrated to be suitable for the fabrication of gradient refractive index (GRIN) micro-lenses<sup>[61]</sup> and waveguides<sup>[62]</sup> as presented in Figure 3d.<sup>[60]</sup>

The same control over the laser intensity can result in a different modality that significantly reduces the fabrication time and improves the surface quality. A change in the fabrication laser intensity leads to a change in the focal volume, changing the voxel size, hence enabling higher accuracy for edges and borders of the 3D structures. This fabrication modality is called two-photon grayscale lithography (2GL), which allows higher resolution in fewer layers by adapting the voxel size during the fabrication of the structure compared to the equal-sized voxels by traditional MPL as compared in Figure 3c. The implementation of this modality is beneficial for micro-optical applications where high surface quality is required for better optical performance, reducing the manufacturing time.<sup>[60]</sup>

## 4. Single Micro-Optical Elements

Modern photonics technologies demand high-quality, high-precision micro-optics elements that provide more freedom for system design, enabling new functionalities and applications that are not possible with conventional optics. In the early works proposing the fabrication of micro-elements via MPL, researchers focused on creating a toolbox of known optical elements scaled down to the micro-scale. Special attention was paid to the surface quality, as optical applications require elements with features smaller than  $\lambda/20$ .<sup>[63]</sup>

In this section, we summarize the primary refractive, reflective, and diffractive single micro-optical elements fabricated with the MPL process. In addition, we further discuss MPL-fabricated free-form optics, polarization, and waveguides. Most of the presented structures will be recalled in the context of their proposed applications in Section 5.

### 4.1. Refractive Elements

#### 4.1.1. Single Micro-Lenses

Spherical, aspherical, and Fresnel micro-lenses were among the first types of micro-optical elements fabricated with MPL.<sup>[7–9,58]</sup> The development of optimized scanning strategies (see Section 3) allows for obtaining precise and easy tailoring of the lens curvature, and high optical quality. An example of a micro-lens printed by MPL is presented in Figure 4a. The obtained relative error of the lens profile can be less than 0.2%.<sup>[58]</sup>

Interestingly, Xu,<sup>[64]</sup> leveraging the unique shaping capabilities enabled by MPL fabrication, proposed a concave-convex micro-lens consisting of two different high-curvature surfaces that offer more design freedom and minimizes aberrations.

Ristok<sup>[57]</sup> demonstrated the largest singlet lens to date, exhibiting the versatility of fabrication by MPL for optical elements up to the millimetric scale. Components at such a scale require dividing the design into smaller sections of the entire structure, potentially resulting in visible stitches on its surface. Free-of-stitching-defect optical components result from a

single-step exposure fabrication and exhibit a molded glass-like clear appearance.

#### 4.1.2. Free-Form Elements

The versatility of 3D fabrication via MPL permits the fabrication of complex free-form structures. It is possible to manufacture, not only single structures or a combination of known optical elements but innovative and nonconventional free-form components for sophisticated optical applications.

For instance, the logarithmic axicon (LA) is a single optical element that differs from the basic spherical-like lenses, exhibiting large focal depth. The resulting beam can be well approximated to a Besselian transverse intensity distribution and is almost unchanged along its optical axis.<sup>[65]</sup>

More arbitrary structures for light collimation can take advantage of the degree of freedom offered by MPL during fabrication. A structure composed of a dielectric total internal reflecting (TIR) concentrator, with an aspherical lens on top of an LED presented high collimation efficiency of light. Such elements demonstrate that efficient primary optics play a crucial role in the miniaturization of illumination systems<sup>[66]</sup> as the one presented in Figure 4c. Similarly, a monolithic bifocal eight-level zone plate by Jiang<sup>[67]</sup> used its double focus property to collimate light from a laser diode with high spatial coherence, presenting an efficiency higher than 92%.

The ability to control the directivity of light is of interest for several optical applications and is achieved by complex free-form micro-optics. A single double-axial hyperboloidal micro-lens with an asymmetrically divergent output beam takes advantage of its two adjustable focal spots for beam shaping of edge-emitting diode lasers in two directions.<sup>[68]</sup> Likewise, Johlin<sup>[69]</sup> proposed a dielectric micro-lens achieving high directivities for point-sources and nano-wire emitters taking advantage of the flexible 3D design and compatibility of MPL.

#### 4.1.3. Micro-Lens Array

The signal-to-noise ratio of the micro-lens array depends on the area filling factor of the elements. Different patterns for the micro-lens array, such as quadratic,<sup>[58]</sup> hexagonal,<sup>[54,55,58]</sup> horizontal, and vertical slicing strategies have been presented.<sup>[70]</sup> One of the main goals is to achieve a full-filling factor; 100% was reached by Wu<sup>[26]</sup> as presented in Figure 4b.

MPL flexibility permits a nonuniform curvature<sup>[71]</sup> and height<sup>[72]</sup> on the micro-lens arrays, as well as multi-lens objectives,<sup>[28]</sup> as presented in Figure 4i, in a single-step fabrication.

### 4.2. Reflective Elements

The advantages of reflective compared to refractive optical designs are the intrinsic achromaticity and compactness. If the designed reflection angle satisfies the condition for TIR with the used photopolymer, then it is possible to obtain an all-dielectric reflector in a single-step fabrication. Alternatively,

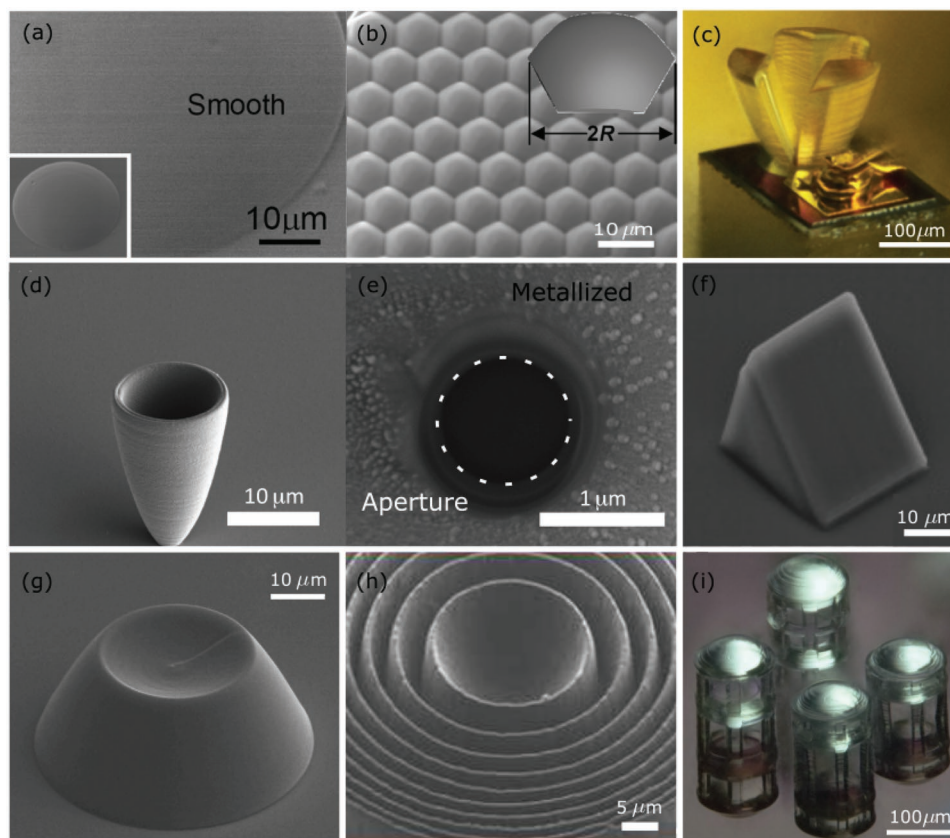


**Figure 4.** a) Single micro-lens and b) close-packed high NA hexagonal micro-lens array. c) On-chip free-form collimator lens. d) (Oblique view) Parabolic reflector coated with Ag and e) (top view) close-up of light aperture etched with a focused ion beam. f) Micro-prism of photosensitive silicon-based composite, highly loaded with Ge isopropoxide. g) Parabolic micro-reflector covering the core of a multimode fiber. h) Central part of kinoform lens. i) Array of a compound micro-lens system for foveated imaging on-chip. a,b) Adapted with permission.<sup>[26]</sup> Copyright 2010, American Institute of Physics. c) Adapted with permission.<sup>[66]</sup> Copyright 2016, The Optical Society. d,e) Adapted with permission.<sup>[27]</sup> Copyright 2011, American Institute of Physics. f) Adapted with permission.<sup>[23]</sup> Copyright 2012, Elsevier Ltd. g) Adapted with permission.<sup>[78]</sup> Copyright 2013, The Optical Society. h) Adapted with permission.<sup>[91]</sup> Copyright 2018, Wiley-VCH. i) Adapted with permission.<sup>[28]</sup> Copyright 2017, Elsevier Ltd.

in a second fabrication step, a metallic coating can be deposited on top of the 3D printed micro-optical element to create reflective-like components.

#### 4.2.1. TIR Reflectors

For a polymerized material with an  $n$  of 1.5, the TIR condition at the interface with the air is satisfied for incidence angles above  $41 \text{ deg}$ , which includes  $45 \text{ deg}$  that is relevant for many applications as it allows right-angle steering of the beam. For instance,  $45 \text{ deg}$  prisms can be fabricated from hybrid materials,<sup>[23]</sup> as presented in Figure 4f, and TIR mirrors combined with micro-lenses were used for out-of-plane coupling between optical fibers and photonic circuits, exhibiting low coupling losses.<sup>[73–75]</sup> A miniature Otto prism was presented as an alternative for out-of-plane coupling via TIR, to excite Bloch surface waves in 1D photonic crystals.<sup>[76]</sup> TIR beam deflectors were implemented in a fully integrated system on fiber, achieving stable 3D-trapping optimized for single cells.<sup>[77]</sup> On the other hand, Bianchi<sup>[78]</sup> used a parabolic reflective design, shown in Figure 4g, to increase the NA of multimode fibers and achieve a focusing power independent of the

immersion medium. In another example, free-form focusing TIR reflectors were used for on-chip optical trapping.<sup>[79]</sup>

Optical designs which feature both refractive and reflective components are called catadioptric designs. They are of particular interest because they can collect light with high-NA. One example is a design with light coming from isotropic point emitters.<sup>[80]</sup> A high NA thin lens presented by Bertoncini,<sup>[19]</sup> based on this catadioptric design, can replace a bulky high-NA aperture microscope objective for forwarding signal collection in point-scanning microscopies.

#### 4.2.2. Metal-Coated Reflectors

Some applications demand an incident angle on the optical component that does not satisfy the TIR condition. This can happen if the incidence angles are close to normal or if the surrounding material has an  $n$  higher than air (e.g., water). One solution is to apply a metallic coating on the micro-structures to provide the required reflective condition. The leading technique to achieve a smooth metallic coating is physical vapor deposition, such as sputtering by evaporation.



Atwater<sup>[27]</sup> proposed a micro-phonic parabolic Ag-coated structure as a light director to produce collimated beams presented in Figure 4d,e. Likewise, a micromirror together with a microlens creates a counter-propagating system to enhance fluorescence signal collection.<sup>[81]</sup> Similarly, a parabolic micromirror is created by depositing an Au layer structure using thermal evaporation-assisted deposition onto a photoresist mold and is used to focus light for sensing applications.<sup>[82]</sup>

In some cases, a metallic coating is required only in a specific area of the micro-structure, to retain both transparent and reflective parts in the final device. Bertocini<sup>[83]</sup> developed a dual-step 3D printing strategy to achieve selective metallization of the slanted face of a 45 deg mirror for the realization of a counter-propagating optical trapping device. Another challenge for mirror-like structures is to achieve uniform metallic deposition on shadowed surfaces or inside cavities. Williams<sup>[84]</sup> addressed this challenge while creating a resonant cavity with metal-coated mirrors by printing one part of the structure connected with a hinge. In this way, the two surfaces that are to be metal coated were exposed and facing the same direction during the metallic deposition. After the deposition process, the hinged mirror was closed with a micro-manipulator to form the resonant cavity.

#### 4.3. Diffractive Elements

Novel optical systems take advantage of the properties of diffractive optical elements (DOE) to create efficient light transformation devices. Unlike their refractive counterparts, DOEs consist of different zones. These zones in the optical element diffract light, resulting in an interference effect that creates the final image by a coherent superposition of light. DOEs are typically fabricated by 2D lithography techniques that limit their topographies. The 3D flexibility and submicron precision in the fabrication of the MPL technique overcomes this limitation.<sup>[85]</sup>

This fabrication technology allows for the creation of micro-structures encoded with gray-level information<sup>[86]</sup> as well as kinoforms,<sup>[87]</sup> which are phase-type diffractive lenses with high diffraction efficiency. Phase-type and multi-level structures, for example, have been shown to enhance the diffractive efficiency of fractal zone plates and demonstrate multiple foci along the optical axis.<sup>[88]</sup> Another example is Dammann gratings, a binary-phase Fourier hologram that generates an array of coherent spot sources.<sup>[89]</sup> Binary radial DOEs are also used to create the so-called “light bottles” starting from a Gaussian beam.<sup>[56]</sup> Similarly, the fabrication of four-level micro-relief DOE exhibits the capability of multi-level fabrication with submicrometer precision by MPL required for DOEs.<sup>[90]</sup>

Similarly, Figure 4h shows a kinoform lens that presents a challenging parabolic profile which has been achieved by MPL. Such elements allow high performance in focusing and high control of X-ray wavefronts.<sup>[91]</sup> Additionally, an inverse-designed thin circular grating-like structure was fabricated on top of a fiber for wavefront modifications. The metal-lens element has the capability of transforming the wavefront from parabolic to spherical at the near-infrared wavelengths.<sup>[92]</sup> Recently, stacked DOEs appeared as a solution to correct field-dependent aberrations

presented in planar lenses, taking advantage of the 3D fabrication capabilities of MPL.<sup>[93]</sup>

Fabrication of a micro-lens array of DOEs is also possible via MPL. An array of continuous surface Fresnel micro-lenses by 3D focal field engineering has been presented. To improve fabrication speed, the fabrication was performed on the Y–Z plane and along the X-direction to have higher control of the structure height.<sup>[94]</sup>

#### 4.4. Polarization Elements

Conventional optical devices for polarization control are based upon intrinsic material properties. Examples include birefringent crystals (e.g., waveplates) or conductive materials (e.g., wire-grid polarizers). However, in the context of 3D printed micro-optics, the material is typically dielectric and non-birefringent. Thus, the main strategies to control the polarization are not based on the material's properties but instead on three out of the four optical phenomena we previously covered: refraction, reflection, and diffraction.

Figure 5a shows an example of a refractive configuration is an integrated micro-optical component on a fiber facet formed by a prism and a grating, proposed by Hahn.<sup>[95]</sup> The refractive element deflects the output of the single-mode fiber by TIR to a polarization-dependent sub-wavelength grating that splits the polarization components.<sup>[95]</sup>

On the other hand, a diffractive element works as a free-form polarization beam splitter for in-plane light manipulation shown in Figure 5b. It functions as free space broadband in the near-infrared beam splitter, splitting the parallel and perpendicular polarizations into different diffraction orders.<sup>[96]</sup>

Another micro-size diffractive element used for polarization control is a grating fabricated through a liquid crystalline polymer by Zanotto (2019).<sup>[97]</sup> The device achieves a photonic response by a refractive index change and the shape of the grating elements by a molecular rearrangement, resulting in a nontrivial polarization state management over multiple beams due to the material anisotropy. With polarization modulation of the diffracted beam, the transmitted beam also experiences a polarization modulation simultaneously, achieving independent control over the polarization and amplitude of different beam channels.

Birefringent optical retarders, instead, are made of dielectric metasurfaces, for which polarization conversion was reported.<sup>[98]</sup> Their efficiency can be improved more than ten times by stacking multiple individual layers into an assembled 3D optical component.<sup>[20]</sup> It is possible to obtain multimodal interference from a 3D printed birefringent dual-core based on a photonic crystal fiber (PCF) design to create a wave-guided polarization splitting device.<sup>[99]</sup> Alternatively, highly birefringent channel waveguides can rotate the polarization by adiabatically twisting them. By controlling the twisting angle of the waveguide, the polarization state changes to an arbitrary or intended state,<sup>[100]</sup> allowing the creation of polarization rotator<sup>[101]</sup> as presented in Figure 5c. A polarization rotator based on the same operation mode has been demonstrated on fiber-to-chip connections, in order to convert TM to TE polarization mode.<sup>[102]</sup>



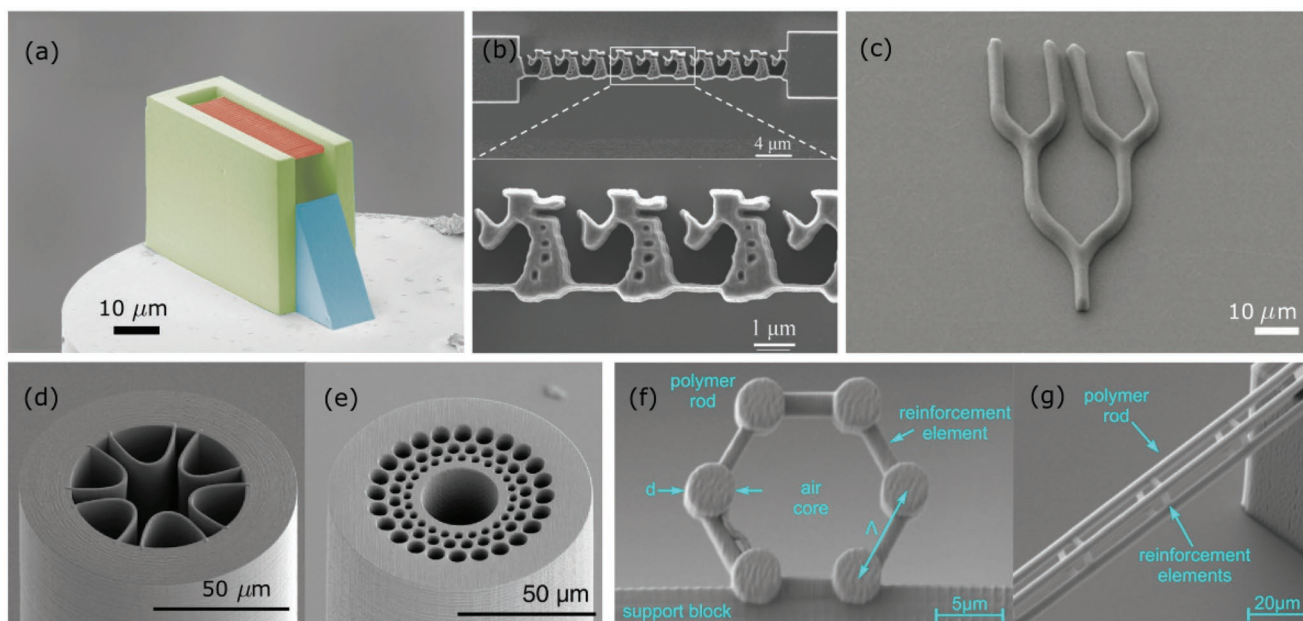


**Figure 5.** a) Polarizer beam splitter composed of a prism highlighted in blue, the lamellar grating in red, and the supporting structure in green. b) Free-form inverse-designed PBS in the near-infrared range with ten periods and  $30\ \mu\text{m}$  length. c) Polarization router via twisted waveguide based on adiabatic mode conversion. d) Anti-resonant hollow-core, and e) fractal ring-core PCF designs. f) Cross section, and g) top view of hollow-core light cage with six strands of  $1\ \text{cm}$  length.<sup>[105]</sup> a) Adapted with permission.<sup>[95]</sup> Copyright 2018, The Optical Society. b) Adapted with permission.<sup>[96]</sup> Copyright 2019, Wiley-VCH. c) Adapted with permission.<sup>[101]</sup> Copyright 2019, Wiley-VCH. d,e) Adapted with permission.<sup>[99]</sup> Copyright 2020, The Optical Society. f,g) Adapted with permission.<sup>[105]</sup> Copyright 2019, American Chemical Society.

Another relevant operation in polarization control is the conversion of the polarized light into different polarization states. Bertoni<sup>[103]</sup> created a linear to circular broadband polarization converter based on a miniaturized Fresnel Rhomb. Here, two reflections at a precise angle create a quarter-wave phase delay between two orthogonal polarization, generating a circularly polarized state. Staking two Fresnel Rhombs achieves half-wave retardation, hence rotating the polarization by  $90\ \text{deg}$ .

#### 4.5. Waveguides

The unprecedented degree of freedom offered by MPL fabrication has been harnessed to fabricate complex optical waveguide configurations based on different approaches. In the first approach, the waveguide cores are MPL fabricated with the capability to create 2D/3D trajectories. The printed cores typically have lateral dimensions in the order of the wavelength to obtain single-mode waveguides and are eventually embedded in a low-index cladding material added in a second step. This has contributed to compelling applications in optical interconnects, which is reviewed in Section 5.5.

In a second approach, MPL was used for the fabrication of waveguides with PCF geometries as presented in Figure 5d,e.<sup>[99,104]</sup> This approach takes advantage of the single-material configuration of PCF fibers and of the vast catalog of waveguide optical properties obtainable by varying the geometry of their longitudinal holes. In a third approach, Jain<sup>[105]</sup> proposed the so-called “light cage” hollow-core waveguides shown in Figure 5f,g. Here, the anti-resonant properties of the longitudinal bars arranged in a circular pattern allow light to be confined in a

hollow waveguide that is highly permeable, with clear advantages for sensing applications.<sup>[106]</sup> In the last approach, MPL is used to fabricate solid-core waveguides by polymerizing materials with two different  $n$  for the core and the cladding areas. This can be performed in two ways: 1) using two different photoresists, one for the core and one for the cladding,<sup>[107]</sup> or 2) by controlling the degree of polymerization (cross-linking), hence its  $n$ , of a single photoresist.<sup>[62,108–111]</sup>

## 5. Applications

### 5.1. Structured Beams—Vortex Beam Generators

A particular beam shape that differs from the classical Gaussian beam may be required for certain applications. One example is the so-called vortex beam that carry orbital angular momentum (OAM), which typically has a ring-shape. The light field is endowed with an on-axis phase singularity, corresponding to a local azimuthal phase dependence of the electric field in an exponential form depending on the topological charge and the azimuthal angle.

Various strategies are used to generate OAM beams in optical applications, several of which have been scaled to micro-size with the help of the MPL process. The most common vortex beam generator architecture is the spiral phase plate (SPP), characterized by a helically increasing optical thickness designed for a specific wavelength. Micro-size single SPPs over a glass substrate,<sup>[112]</sup> and on a single-mode fiber,<sup>[113]</sup> have been presented. OAM beams have the potential to become a platform for optical communication systems since these beams give

access to an infinite number of states and due to the orthogonality of distinct azimuthal modes. Therefore, the purity of the OAM modes is of high importance. Stegenburgs<sup>[114]</sup> demonstrated the fabrication of SPP to generate high-purity OAM beams, measured through modal decomposition, and tested them in an optical communication setup to convey data signals.

More recently, DOEs have been incorporated to realize complex illumination patterns, for example to generate structured light from purely geometrical phase transformations. Spin-to-orbital optical angular momentum converters with space-variant grating have been demonstrated by Wang,<sup>[98]</sup> as well as a diffractive phase plate for spatial intensity beam shaping with sub-micrometer features by Gissibl.<sup>[12]</sup> Schmidt<sup>[115]</sup> proposed a free-form hologram with a design methodology for smooth and uniform phase profiles, and Oliveira<sup>[116]</sup> proposed a DOE to generate a superposition of high-order Bessel beams with a controlled number of rings, showing the incorporation of diffractive elements to complex designs.

A combination of different elements can generate vortex beams with unusual characteristics. Žukauskas<sup>[117]</sup> combined a generic SPP with an axicon to produce pseudo-nondiffracting high-order optical vortex beams, and Tian<sup>[118]</sup> combined an SPP with a lens for high-order focused vortex beams. Unconventional structures can also generate OAM beams, for example, the wrinkled axicons presented in **Figure 6a,b** by Sanchez-Padilla.<sup>[29]</sup> The structures can generate optical vortices from spin-orbit interactions associated with nonparaxiality by using hypocycloid and epicycloid curves on axicons.

On the other hand, alternative flat optics methods can generate high-order OAM beams. Balcytis<sup>[119]</sup> demonstrated tightly focused vortex beams in a single wavefront transformation by a binary spiral zone pattern based on a high numerical aperture

micro-lens fabricated with a combination of MPL and focused ion beam (FIB) milling. Wang<sup>[98]</sup> proposed a spin-to-OAM coupler from a space-variant birefringent structure. Simultaneously, wavelength and OAM multiplexing/demultiplexing were possible using a new on-chip micro-component consisting of a tunable MEMS-based Fabry-Perot filter, together with an SPP.<sup>[120]</sup> Another example is an optical vortex generator called a mirror-rotation-symmetrical single-focus spiral zone plate (MS-SZP). This element is a combination of an SPP with a Gabor zone plate and generates single-focus optical vortex beam with OAM.<sup>[121]</sup>

Multiple OAM beams can be generated simultaneously with a single device. Hu<sup>[122]</sup> proposed a multifocal logarithmic axicon, together with a multizone spiral phase plate, for independent control of phase division of multiple OAM output beams. Optical vortex beams can be carriers of information in optical communications; due to their spatial orthogonality; these beams can be multiplexed and demultiplexed. Lightman<sup>[13]</sup> proposed a vortex mode sorter with optimized profiles and distance between the elements handling both pure and mixed vortex beams, for low-order OAM. On the other hand, inspired by the concept of lab-on-fiber, Xie<sup>[123]</sup> demonstrated the integration of a fork-type polymer vortex grating for (de)multiplexing on facets of a few-mode fiber. Such an OAM (de)multiplexer enables the direct conversion of multiple OAM states of different orders within the optical fiber back to Gaussian-like beams in a different direction in the output facet.

Alternatively, taking advantage of a hybrid micro-optical component, an increase of five times the propagation of a Bessel beam was employed by mode field expansion.<sup>[124]</sup>

Furthermore, Sokolovskii<sup>[125]</sup> developed a solution to the beam-quality problem presented in diode laser by fabricating

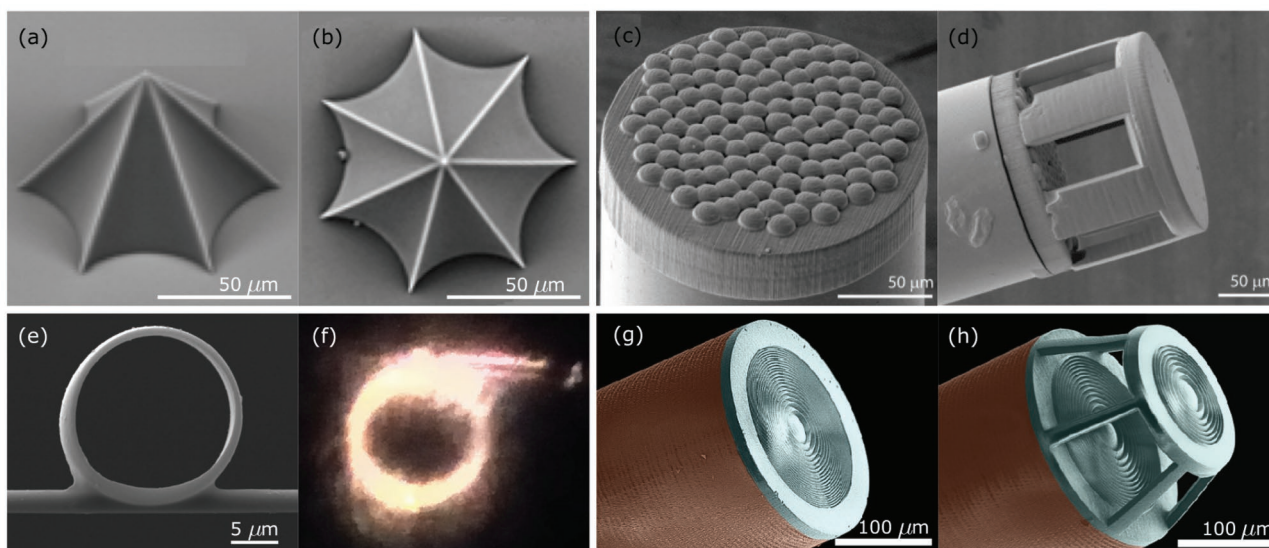


**Figure 6.** Hypocycloidal and epicycloidal axicons for Bessel beam generation: a) oblique incident view and b) top view. c) Microlens array and d) entire hyper-telescope on a multi-core fiber bundle for two-photon imaging. e) 20  $\mu\text{m}$  diameter micro-ring resonators on optical fiber taper, and f) optical microscope image of a micro-ring being excited using white light. Diffractive Fresnel lenses on single-mode fibers for dual-fiber optical trapping with g) NA = 0.5 and h) NA = 0.7. a,b) Adapted with permission.<sup>[29]</sup> Copyright 2016, The Optical Society. c,d) Adapted with permission.<sup>[31]</sup> Copyright 2021, The Optical Society. e,f) From the Authors Dr. V. Melissinaki and Dr. M. Farsari with their kind permission to reuse it for this review.<sup>[136]</sup> g,h) Adapted with permission.<sup>[137]</sup> Copyright 2019, American Chemical Society.

an axicon for Bessel beam generation with super focusing and high- $M^2$ . This approach achieved an order of magnitude reduction in the size of the focal spot and performed the optical trapping of red blood cells. Meanwhile, Reddy<sup>[126]</sup> recently presented a unified approach to generate zeroth and high-order Bessel beams from single-mode optical fibers.

## 5.2. Imaging Systems

The use of bulky optical elements, due to the limitations of traditional optics manufacturing methods, has long hindered the miniaturization of imaging systems and the realization of ultra-thin micro-endoscopes.

As presented in the previous sections, MPL can fabricate micro-size optics with high precision; thus, the realization of high-performance complex micro-optical systems and microlens arrays<sup>[127]</sup> for imaging has become possible. Moreover, the unprecedented capability of MPL to create arbitrary shapes provides substantial potential for aberration correction. Gissibl<sup>[128]</sup> presented singlet, doublet, and triplet lenses optimized to correct for monochromatic aberrations during the design phase. The authors showed the use of these multi-lens objectives directly printed on CMOS sensors and the facet of a multicore optical imaging fiber. On the other hand, a combination of diffractive and refractive elements and two different photoresists has been used to correct chromatic aberrations to realize achromatic and apochromatic microlenses.<sup>[21]</sup>

An endoscopic probe composed of a cascade of microlenses with aspheric profiles allowed to achieve high numerical apertures and control aberrations resulting in high spatial resolution (1  $\mu\text{m}$ ).<sup>[129]</sup> Wang<sup>[130]</sup> presented another application of aspherical microlenses, fabricating a high-NA singlet lens on a fiber-facet to collect the fluorescence signal of an analyzed sample. Aspheric microlenses were also presented for correcting optical aberrations of minimally invasive GRIN micro-objectives, obtaining an extended field of view and demonstrating its use for imaging deep brain regions.<sup>[131]</sup> In another application for endoscopy, a miniaturized coherent beam combiner presented in Figure 6c,d, including a 120-micro-lens array at the tip of an ultra-thin multicore fiber, demonstrated an efficiency increase of  $\times 35$  in performing two-photon imaging.<sup>[31]</sup>

For application in optical coherence tomography, a fiber probe was realized by fabricating a miniaturized optical system containing an off-axis paraboloidal TIR surface.<sup>[132]</sup> More recently, Li<sup>[133]</sup> developed novel side-facing free-form micro-optics on single-mode fibers, resulting in an aberration-corrected optical coherence tomography probe. In this study, the use of this structure was demonstrated in mouse thoracic arteries, where biologically relevant microstructures were visualized up to 500  $\mu\text{m}$  deep into the tissue.

However, different modalities have conflicting optical requirements; for example, the NA required for high sensitivity fluorescence measurements is higher than that required for optical coherence tomography. An optimized lens-in-lens design contains optical surfaces that address the need for optical design for both modalities, a combination of TIR mirrors and lenses whose fabrication is only possible via MPL.<sup>[134]</sup>

Yanny<sup>[135]</sup> fabricated a phase mask consisting of an array of multi-focal nonuniformly spaced microlenses for single-shot 3D fluorescence microscopy. The phase mask was placed in the Fourier plane of the GRIN objective lens of a miniature wide-field fluorescence microscope to encode the 3D fluorescence intensity distribution into a single 2D measurement.

Light-blocking features are also important in multi-element imaging systems, as they integrate apertures that maximize imaging quality. Toulouse<sup>[138]</sup> proposed a new method to create nontransparent micro-optics components by integrating super-fine inject printing into the optical systems. However, an aperture stop created with this method cannot be integrated into all optical systems, as it requires enough space to incorporate the ink mold.

More recently, Weber<sup>[139]</sup> proposed an alternative approach to creating thin and completely nontransparent aperture stops based on shadow evaporation and used it to demonstrate a multi-element wide-angle Hypergon micro-objective.

A miniature direct spectrometer for visible light, including MPL-fabricated imaging, diffractive, and light-blocking micro-optical elements, was recently presented, featuring a volume of  $100 \times 100 \times 300 \mu\text{m}^3$ .<sup>[140]</sup> This footprint is at least two orders of magnitude smaller than currently available direct spectrometers. This presented miniaturized optical system illustrates the strengths of MPL: the possibility of creating multiple free-form surfaces, including asymmetrical and highly tilted surfaces, their inherent near-perfect alignment, and the integration of optical apertures.

A combination of free-form stacked lens systems and light-blocking elements has also been used to implement an ultra-compact multi-aperture wide-angle ( $180^\circ \times 360^\circ$ ) camera.<sup>[141]</sup>

## 5.3. Optical Manipulation—Optical Tweezers

Optical tweezers (OT) are contactless tools that trap and manipulate microparticles using light beams.<sup>[142]</sup> Implementing OT generally requires special light fields, constituted of either a single high NA beam or by low NA counter-propagating beams, which are created with complex and bulky setups. MPL fabrication has proved to be a powerful method to create complex light fields at the microscale, allowing the miniaturization of those optical setups. Libérale<sup>[77]</sup> used MPL to fabricate a set of micro-prisms on a four-fiber bundle, in which cores were distributed according to an annular geometry. The output beams were deflected by TIR to converge with high NA at a common spot, creating a fiber-based 3D optical trap. The system was integrated into a microfluidic system for stably trapping tumor cells while simultaneously recording their Raman signature.

More recently, Plidschun<sup>[143]</sup> proposed a high NA meta-lens to tightly focus the expanded Gaussian beam from a single-mode fiber and demonstrated efficient 3D trapping of microbeads and bacteria.

In another fiber-based approach, Asadollahbaik<sup>[137]</sup> used MPL-fabricated diffractive Fresnel lenses on the facets of a pair of optical fibers to create counter-propagating beam optical traps presented in Figure 6g,h. The converging beams resulted in strong trapping efficiency in both the axial and transverse directions, allowing the stable trapping of particles as small as 500 nm at low laser power. Using this dual-fiber configuration,



the same research group studied the emission of trapped photoluminescent nanorods<sup>[144]</sup> and the vitality of single algal cells.<sup>[145]</sup>

A miniaturized on-chip dual-beam trapping configuration was also proposed by Yu.<sup>[79]</sup> Their approach was based on the MPL fabrication of free-form micro-optics on the end faces of optical waveguides and was designed to trap and manipulate suspended particles in an integrated chip-scale platform.

#### 5.4. Optical Sensing

Uncommon micro-optical elements designed for sensing applications take advantage of the flexibility of the MPL process for its implementation in optical fiber facets and multiple devices. Microcavities integrated with different optics have been implemented on optical fibers for lab-on-fiber sensing applications. For example, the architecture of a Fabry–Perot optical resonator is exploited for sensing applications, since it allows the formation of a small cavity where gases are trapped. The cavity detects the  $n$ , or absorption changes, allowing its use as a vapor sensor.<sup>[146,147]</sup> Due to the thermal expansion and thermoelastic effect, the  $n$  of the sensing material changes by altering the background temperature. It results in a wavelength shift of the flat Fabry–Perot resonant, permitting its use as a thermal radiation sensor.<sup>[148]</sup> This temperature-dependent optical response was improved by using a reflective and curved surface, as presented by Williams.<sup>[149]</sup> On the other hand, a magnetic field sensor can result from bounding nano iron particles to an FP resonator, as reported by Gorau.<sup>[150]</sup> Some well-known optical phenomena like Moiré patterns were realized at the microscale by forming a grating-like deformable and rigid polymeric structure.<sup>[151]</sup> This was shown to serve as a passive fluidic micro-sensor with an all-optical readout.

Moreover, other particular geometries are possible for various fiber tip sensing applications. A whispering gallery microcavity with high-quality factors investigates volatile organic compounds showing high sensitivity and a fast time response.<sup>[152]</sup> Subsequently, Liu<sup>[153]</sup> presented integrated micro-ring resonators in 3D space for sensing organic vapors, demonstrating satisfactory reversibility since there is no chemical reaction between the volatile organic compounds and the photoresist.<sup>[153]</sup> Similarly, Figure 6e,f shows microrings on fiber tapers which were used as ethanol vapor sensors based on reversible physisorption effects. The results support a new type of photonic platform exhibiting unique guiding performance and modal interaction characteristics.<sup>[136]</sup> In another example, Zhang<sup>[154]</sup> introduced an optofluidic Mach–Zehnder interferometer with a hollow cavity. This microsystem resulted in a promising platform for refractive index measurements of analytes. Alternatively, a combination of a parabolic mirror and a surface-enhanced Raman scattering was realized on a fiber facet as a radar-like design sensor, exhibiting a higher SERS effect for excitation in the visible spectral range.<sup>[82]</sup> Furthermore, an optical force sensor was created from four polymer plates in a force-sensitive micro-gripper. The optical force from the fiber displaces the sensing plates, and the differences in path length between the light reflected from different plates leads to interference effects used to predict the axial compression of the monolithic micro-gripper.<sup>[155]</sup>

On the other hand, the confinement and diffusion capabilities in the hollow cores of microstructured waveguides are of interest for sensing applications. A PCF-like structure was shown to track and analyze individual diffusion of nanoscale objects in a water medium. This was done by studying the particle's Brownian motion as retrieved by analyzing the elastically scattered light from the core mode and using standard tracking algorithms and mean squared displacement analysis with fair accuracy.<sup>[156]</sup> Another possibility is the integration of the hollow-core light cage interfacing optical fibers for on-chip waveguides for sensing applications. The system's sensing ability was demonstrated by examining ammonia using a tunable diode laser absorption spectroscopy.<sup>[106]</sup>

##### 5.4.1. Scanning Probe Microscopy

The potential of 3D printed micro-optics was presented by Dietrich,<sup>[157]</sup> who engineered a 3D printed scanning probe microscope on top of a four-fiber array. In this work, the cantilever's actuation is performed optically by the opto-thermal expansion of a portion of the cantilever thanks to a beam coming from the first fiber, and is deflected by two TIR mirrors that are part of the cantilever. The position is interferometrically read through a cavity formed by a free-form mirror on the bottom of the cantilever and the facet of a second fiber. The near field probe's optical excitation comes from the fourth fiber, whose beam is focused and deflected with a free-form metallic mirror. Finally, the signal coming from the metallic tip is collected into the third fiber with a free-form micro-lens.

Zou<sup>[158]</sup> presented a novel fiber-tip polymer clamped-beam probe for micro-force sensor. The force-sensing probe exhibits high force sensitivity with the smallest force-detection limit in direct contact mode reported until now.

#### 5.5. Optical Communications—Photonic Circuits

Harnessing the full potential of integrated photonic circuits requires the availability of 3D intra-chip and chip-to-chip optical interconnects, easy coupling between out-of-plane elements and planar elements fabricated with 2D lithographic technologies, and efficient coupling between optical fibers and on-chip photonic systems, to name just a few.

The first proposal of MPL-made suspended-core (or free-standing) optical waveguides as an interconnect between different optical fibers was presented in 2005.<sup>[159]</sup> More recently, this approach was used in the so-called “photonic wire bonding” paradigm, allowing the creation of chip-to-chip optical interconnects and between different types of conventional waveguides, such as optical fibers and photonic chips,<sup>[14,160–162]</sup> as the example presented in **Figure 7a**. Schumann<sup>[100]</sup> introduced a hybrid device with 2D and 3D elements fabricated by MPL, which demonstrated the efficient coupling from a planar to a 3D bridge waveguide and a whispering gallery mode resonator, as well as a broadband mode-evolution-based polarization rotator. Free-standing MPL-fabricated single-mode waveguides were used to obtain out-of-plane couplers, for coupling light into and out of on-chip planar waveguides,<sup>[59,163]</sup> as well as waveguide over-passes for nonplanar topologies.<sup>[164]</sup> Nocentini<sup>[165]</sup> introduced



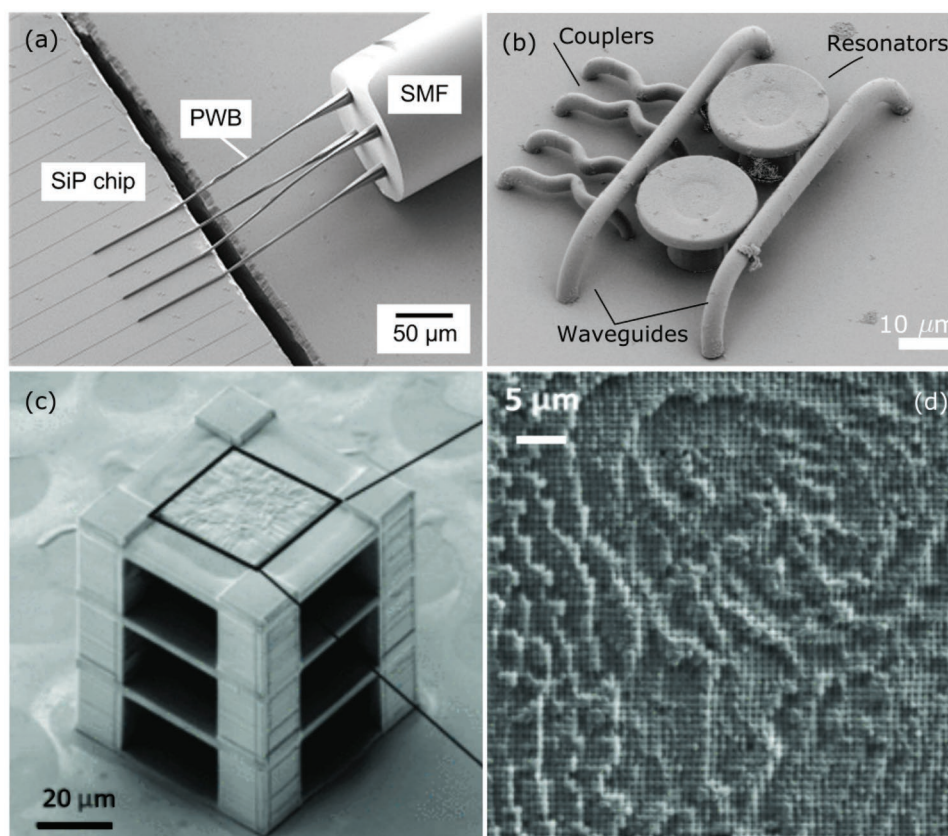


**Figure 7.** a) Fiber-to-chip connection using photonic wire bonding. b) 3D quantum optical assembly of waveguides, couplers, and micro-disk resonators for single-photon generation. c) Full view and d) close-up of array of pixels with radius 850 nm and height between 0.4 and 0.5  $\mu\text{m}$  for support of ANN. a) Adapted with permission.<sup>[162]</sup> Copyright 2018, The Optical Society. b) Adapted with permission.<sup>[169]</sup> Copyright 2013, Nature Publishing. c, d) From the Author Dr. E. Goi with her permission to reuse it for this review.<sup>[178]</sup>

dynamic control of spectral properties of optical elements by using a combination of both rigid and tunable elastic polymers. They integrated waveguides, grating couplers, and whispering gallery mode resonators on a photonic chip that can be actuated and controlled by a remote and noninvasive light stimulus.

Integration of photonic chips into hybrid photonic devices requires high-precision alignment and adaptation of optical mode profiles. To overcome these challenges, Dietrich<sup>[73]</sup> presented free-form, TIR, and multi-lens optics printed on the facet of photonic chips and optical fibers reducing alignment tolerances in passive assembly and efficient adaptation of different beam profiles. The integration of a microlens and an out-of-plane bent polymer waveguide was also presented to create a low-loss fiber-to-chip broadband and a near-adiabatic coupler.<sup>[166]</sup>

Alternatively, optical tapers with PCF-like segments fabricated on top of optical fibers were used to rescale the fiber mode size to allow efficient direct coupling between different elements,<sup>[30]</sup> as mode expanding tapered waveguides to relax coupling alignment tolerances between fibers,<sup>[167]</sup> and to maximize the coupling efficiency to chip connections.<sup>[104]</sup>

Trappen<sup>[75]</sup> addressed wafer-level probing of edge-coupled photonic integrated circuits by presenting MPL-fabricated free-form coupling elements that fit into deep-etched dicing trenches on the wafer surface. In this case, the coupling element comprises a TIR mirror for redirecting light from an out-of-plane to an in-

plane direction and uses an aspherical lens for a mode-field match with the waveguide. Several different combinations of waveguide facets and coupling elements proved the high reproducibility of the low coupling loss of the devices. 3D-printed fiber sockets were proposed for plug-and-play micro-optics, exploiting the LDW fabrication flexibility and reducing the alignment issue<sup>[168]</sup> This was proven for telecom wavelengths, but it is likely that it will be extended to different platforms and for various applications.

## 5.6. Quantum Technology

On-chip photonic circuits working at a single-quantum level play an important role in future quantum information processing. Photonic elements like photonic crystals, resonators, and waveguides are fundamental photonics entities required to assemble quantum photonic devices. Schell<sup>[169]</sup> fabricated a combined structure with interconnects and functional elements, such as resonators and emitters as presented in Figure 7b, from a photoresist containing nanodiamonds including nitrogen vacancy-centers. The device evidenced active quantum functionality for single-photon generation, as well as subsequent collection and routing via a waveguide.

Single-photon sources with high photon-extraction efficiency are crucial building blocks for photonic quantum applications.

Self-assembled semiconductor quantum dot (QD) sources are of interest because they allow the generation of single-photon states with suppression of multiphoton events. With these sources, broadband extraction and shaping of their output to match acceptance angles of different light-collecting optics are required. To address these challenges, Fischbach<sup>[170]</sup> proposed a quantum light source with a broadband extraction efficiency of up to 40% and excellent single-photon purity and the capability to transfer quantum light to external optics. The device was fabricated by combining 3D electron-beam lithography to realize a QD micro-lens and MPL to create an optimized high-NA micro-objective integrated with the single-photon source.

This approach was further developed toward an efficient coupling (up to 26%) of single-photon sources to single-mode fibers by fabricating a TIR solid immersion lens and a coupling lens on the fiber facet.<sup>[80,171]</sup>

On the other hand, quantum emitters can be directly embedded in MPL-fabricated polymer waveguides.<sup>[172,173]</sup> The advantage of this is that it simplifies the configuration for excitation and efficient collection of single photons.

Additionally, electromagnetically-induced transparency (EIT) was observed on “light cage” structures, proving it to be a basis for a manifold of quantum-storage and quantum-nonlinear applications as a vapor-based photon delay.<sup>[174]</sup>

### 5.7. Machine Learning

The use of machine learning in different optical applications has led to new tools for the optimization of optical devices. One demonstration of artificial intelligence in optics is that of Goi,<sup>[175]</sup> who proposed a nano-imager for a multilayered artificial network (ANN) formed by passive diffractive layers that work in collaboration to perform handwritten digit classification. Furthermore, Ren<sup>[176]</sup> implemented multi-layer perceptron artificial neural networks (MANN) for time-efficient and accurate reconstruction of a 3D vectorial holographic image. The trained MANN produced a pair of phase patterns used to generate the 2D vector fields and a digital phase hologram embedded with a large-angle Fourier transform holographic lens with a 0.8 NA. This approach provides unprecedented wavefront manipulation capabilities of 3D vectorial fields thanks to the design of micro-optical elements by machine learning techniques and their fabrication by MPL.

Nowadays, the demand for communication technology of encrypted information has increased, presenting the need for rigid authentication schemes for a specific decryption key. In large-scale communication systems, the data transfer through optical signals, while the decryption is carried out in the electronic domain. This decryption methodology costs speed in the conversion of information. For this reason, the decryption should be performed directly in the optical domain to fully take advantage of the characteristics of the optical signals, which are the propagation speed and the direct information processing. Considerable effort has focused on developing in optical security schemes, but the encryption and decryption require multiple passes through different bulky optical elements. As an alternative solution for this limitation, Goi<sup>[177]</sup> proposed to employ machine learning based on error back-propagation methods for the generation of compact optical decryptors integrated on complementary

metal-oxide-semiconductor (CMOS) chips. These single-layer holographic perceptrons train to perform decryption of single or whole classes of images and operate in NIR communication wavelengths. Such elements can reach over 500 million neurons per square centimeter while controlling the neuron height precision down to 10 nm, which is allowed by the fabrication via MPL.<sup>[177]</sup> Similarly, interference of optical signals and imperfect optical components are subject to aberrations. Optical neural networks are proposed for aberration detection by retrieving information on phase and light amplitude directly in the optical domain. Figure 7c-d shows multilayered perceptrons printed by MPL are presented as aberration detectors.<sup>[178]</sup>

Moughames<sup>[179]</sup> presented photonic interconnects as complex 3D waveguides for discrete spatial filters as convolutional neural networks for efficient multiplexing of multiple input and output channels. The use of deep neural networks (DNN) can be advantageous for optimizing the designs of optical elements. Panusa (2022)<sup>[180]</sup> designed a tool based on DNN trained with a large synthetic database to reduce the core-to-core spacing of the imaging bundles of rectangular step-index optical waveguides according to the highest reconstruction accuracy. The DNN can improve the imaging resolution of the step-index waveguide by undoing the scrambling due to crosstalk and removing noise from the data. This tool establishes an efficient technique taking advantage of DNN not only for post-processing but also as a design tool.

Alternatively, the machine-assisted deep learning can be exploited for the optimization of the MPL performance itself, for instance, automated detection of part quality while monitoring the LDW process. Light dosage adjustment can be achieved of up to 95% with  $\leq 2$  ms response time.<sup>[181]</sup> This issue is emerging as the fabrication throughput of the technology is increasing, but the users' experience and knowledge are relatively low, especially as novel materials are being introduced.

## 6. Materials and Post-Processing

Historically, acrylate<sup>[7,8]</sup> and epoxy<sup>[44,58]</sup>-based materials were employed for the first fabrication of micro-optics, mainly due to their established ease of use and straightforward applications. Later, hybrid organic–inorganic polymers<sup>[23,182]</sup> were used, which offered more practical structuring, mechanical,  $n$ , and transparency properties required for photonics, while still being convenient for processing. Finally, some distinct high  $n$  (up to 1.62) or high transparency materials for the VIS spectrum were developed for specific optical applications.<sup>[183]</sup> Polymers are useful substances that offer a mix of different monomers and inorganic compounds, thus allowing their properties to be modified by changing their ratios.<sup>[6,11]</sup> Doping with organic and inorganic ingredients also allows further enhancement of their functionalities, including optically active functions.<sup>[184–187]</sup> Precise incorporation of quantum dots (QD) as a nanoscale integration has also been successfully demonstrated.<sup>[171]</sup> For micro-optics, negative tone resists are most commonly used as they are applied to create free-form complex geometries; however, positive tone resists can also be exploited for concave lenses as well as templating and replication applications. Many of the aforementioned materials optimized for MPL are available commercially: Microresists,

Microchemicals, FORTH-IESL (Nonlinear Lithography Group, Dr. M. Farsari), Nanoscribe, Glassomer, UpNano, and Laser nanoFab. More details on the materials' chemistry, the photopolymerization process, and the properties of the printed substances can be found in the literature.<sup>[6,11,15–17]</sup>

### 6.1. Post-Processing

Metal deposition is the most straightforward approach to make fabricated polymer microstructures reflective. This can be performed nonselectively by direct metal sputtering,<sup>[27]</sup> via selective wet chemistry,<sup>[188]</sup> or using a sacrificial mask.<sup>[189]</sup> Polymer 3D micro-optics were shown to be compatible with atomic layer deposition (ALD) coating technology to dramatically increase their transparency by up to 99%, which is the essential breakthrough toward manufacturing stacked multi-layer components.<sup>[190]</sup> The latest advance in the material front is a high-temperature post-treatment known as pyrolysis or calcination of hybrid materials.<sup>[191]</sup> After MPL fabrication and development, evaporation of organic substances (C and H converting into CO<sub>2</sub> and H<sub>2</sub>O) occurs, and the remaining inorganic fraction is sintered while maintaining the predefined geometry. This is a game-changing option, enabling 3D additive manufacturing of inorganic substances at nanoscales,<sup>[192]</sup> including fused silica glass.<sup>[193]</sup> Recent reports showed this to be an efficient route toward the generation of pure crystalline substances of various phases<sup>[194]</sup> as well as the production of glassy micro-optical components.<sup>[25]</sup> This approach achieves sub-100 nm feature dimensions due to isotropic shrinkage of the substance during the calcination/pyrolysis process, which enables additive manufacturing of deep sub-wavelength 3D structures.<sup>[63,194]</sup> When combined with doping of inorganic luminescent compounds (for instance, Eu), free-form architectures for optically active 3D micro-devices can be achieved.<sup>[187,195]</sup>

### 6.2. Replication

Nanoimprint lithography and soft-lithography methods are applied to increase the production rate of MPL-based micro-optical components,<sup>[196]</sup> predominantly for arrays of micro-lenses which are time-consuming to fabricate using LDW serial writing and are simple to multiply using various replication means.<sup>[127]</sup> The initial template can be made of organic or hybrid material and transferred via polydimethylsiloxane mold to virtually any photo- or thermo-crosslinking polymer.<sup>[197]</sup> Even though this method is well known among researchers, in the field and is of crucial importance for the industry, there are only a few dedicated research reports in the literature.<sup>[127,131,196,197]</sup>

### 6.3. Characterization of Performance

The MPL enables rapid, flexible, and scalable production of 3D micro-optics, and the demand for their accurate characterization is growing steadily. Yet, this is hindered by the fact that most of the established characterization techniques are for 2D surfaces or bulky 3D macroscale objects. There is no standard method for proper characterization of *n* at the microscale as all of the

approaches have limitations at this scale with free-form shapes. The exposure dose, the developing procedures, and the drying and aging of the structure, contribute to the local *n*, which in turn modulates the efficient *n* of the functional 3D optical element.<sup>[62,108]</sup> Some solutions of thermal (moderate temperature) or high-temperature post-treatments have been suggested to make *n* uniform across the polymerized volume so that the material “forgets” the exact local exposure.<sup>[25,198]</sup> Although these protocols are helpful for repeatability, the exact *n* and potential induced birefringence (tensions arising due to shrinkage) are still open questions.

For photoresists, the degree of polymerization (cross-linking) influencing the *n* increases with the UV duration and the aging process. Even using mild heat treatment for 1 h at 60 °C is sufficient to noticeably increase the refractive index.<sup>[183]</sup>

### 6.4. Optical Resiliency—Laser-Induced Damage Threshold

A laser-induced damage threshold (LIDT) is typically used to evaluate the optical resiliency of optical components. Thin films, bulky 3D micro-structures, and 3D nano-lattices can have significantly different optical damage thresholds for the same material due to their dramatically different surface, geometry, and surface-to-volume ratios. Studies have compared the various materials that can be structuralized as films by MPL,<sup>[199]</sup> as well as the influence of the presence of photoinitiators,<sup>[200]</sup> observation of micro-lens damage,<sup>[201]</sup> measurement of bulky 3D micro-structures and 3D lattice nano-structures,<sup>[202]</sup> and approval of novel high resilience material.<sup>[203]</sup> However, this is still an evolving research trajectory driven by the demand for calibrated and tested micro-optical devices.

The performance and physical characteristics of micro-optical structures depend mainly on the material properties and the MPL technology employed for their fabrication. Prior knowledge of the refractive index of different photopolymers under exposure to MPL allows greater control over the design for the desired performance of an optical element, as well as the impact on the transparency of the structure. Similarly, knowing the damage threshold and mechanical properties of the fabricated elements can be important for particular applications. Finally, the implementation of active and tunable materials in micro-optical elements has been proposed for novel optical applications. Reported values of the previous properties discussed are presented in **Table 2**.

**Table 2.** Microstructure properties and materials reported in the context of micro-optics.

Refractive index	1.463–1.62 <sup>[183]</sup>
Transparency	90% <sup>[200]</sup> –99 % <sup>[190]</sup> for vis–NIR
Damage threshold	Thin films, = 1–10 J cm <sup>-2</sup> for fs and ns pulses <sup>[200,203]</sup> Woodpiles, = 0.1 J cm <sup>-2</sup> <sup>[202]</sup>
Active optical materials	Organic—Disperse Red, <sup>[204]</sup> R6G, <sup>[184]</sup> Fluorescein, DCM, Coumarin 152 Inorganic—Eu, <sup>[187]</sup> Er, Yb, Tm, <sup>[24]</sup> Nd <sup>[195]</sup>
Tunable materials	Protein bovine serum albumin (BSA) for up to ≈40% length change <sup>[205]</sup>
Mechanical properties	0.44 MPa <sup>[206]</sup> to 4.9 GPa <sup>[207]</sup>



## 7. Summary and Conclusions

Since its emergence 25 years ago, the field of micro-optics has been rapidly expanding, accelerated by the contribution of MPL as a tool for rapid prototyping. Micro-optics has quickly scaled-up with the appearance of dedicated commercial LDW setups, and it is still the most versatile technique for designing, creating, and testing novel materials. It is also a unique tool for complex free-form geometries for 3D micro-optics. In comparison with electron beam lithography or ink-jet printers, MPL ensures a higher-throughput and wider variety of architectures, especially photonic integrated circuits. Most recent advances in active optical compounds, high  $n$ , and high resilience substances enable the additive manufacturing of heavy-duty micro-devices compatible with current existing platforms. Scaling up throughput toward industrial demands is being pushed forward by advancing parallelization and beam-shaping techniques. Combined with replication and post-processing solutions, MPL offers not only polymer micro-optics but also glassy and optically active elements. Methodologies for characterization and new standards for microscale 3D optical components will be an active field of technological research in the near future, which will significantly contribute to the widespread use of laser lithography-made micro-optical elements and assembled components. In summary, the field of micro-optics currently appears to be where MPL finds immediate industrial applications as a mature additive manufacturing technology.

## Acknowledgements

Research Council of Lithuania (project No. S-MIP-20-17) and EU LASERLAB-EUROPE (grant agreement No. 871124, Horizon 2020 research and innovation programme) projects are acknowledged for their financial support of VU LRC. King Abdullah University of Science and Technology baseline funding BAS/1/1064-01-01 is acknowledged for supporting the research group at KAUST.

## Conflict of Interest

The authors declare no conflict of interest.

## Keywords

fiber-optics, integrated devices, laser 3D printing, micro-optics, nanophotonics, nanotechnology, two-photon polymerization

Received: July 21, 2022

Revised: September 16, 2022

Published online: November 27, 2022

- [1] J. H. Strickler, W. Webb, *Opt. Lett.* **1991**, *16*, 1780.  
 [2] S. Maruo, O. Nakamura, S. Kawata, *Opt. Lett.* **1997**, *22*, 132.  
 [3] R. Borisov, G. Dorojkina, N. Koroteev, V. Kozhenkov, S. Magnitskii, D. Malakhov, A. Tarasishin, A. Zheltikov, *Appl Phys B-Lasers O* **1998**, *67*, 765.  
 [4] S. Maruo, J. Fourkas, *Laser Photon. Rev.* **2008**, *2*, 100.

- [5] Y.-L. Zhang, Q.-D. Chen, H. Xia, H.-B. Sun, *Nano Today* **2010**, *5*, 435.  
 [6] M. Malinauskas, M. Farsari, A. Piskarskas, S. Juodkazis, *Phys. Rep.* **2013**, *7*, 1.  
 [7] R. Guo, S. Xiao, X. Zhai, J. Li, A. Xia, W. Huang, *Opt. Express* **2006**, *14*, 810.  
 [8] C. Liberale, G. Cojoc, P. Candeloro, G. Das, F. Gentile, F. D. Angelis, E. D. Fabrizio, *Photon. Technol. Lett.* **2010**, *22*.  
 [9] M. Malinauskas, A. Žukauskas, V. Purlys, K. Belazaras, A. Momot, D. Paipulas, R. Gadonas, A. Piskarskas, H. Gilbergs, A. Gaidukevičiūtė, I. Sakellari, M. Farsari, S. Juodkazis, *J. Opt.* **2010**, *12*, 12.  
 [10] J. Serbin, A. Egbert, A. Ostendorf, B. N. Chichkov, R. Houbertz, G. Domann, J. Schulz, C. Cronauer, L. Fröhlich, M. Popall, *Opt. Lett.* **2003**, *28*, 301.  
 [11] M. Farsari, M. Vamvakaki, B. N. Chichkov, *J. Opt.* **2010**, *12*, 124001.  
 [12] T. Gissibl, S. Thiele, A. Herkommer, H. Giessen, *Nat. Commun.* **2016**, *7*, 11763.  
 [13] S. Lightman, G. Hurvitz, R. Gvishi, A. Arie, *Optica* **2017**, *4*, 605.  
 [14] M. Blaicher, M. Billah, J. Kemal, T. Hoose, P. Marin-Palomo, A. Hofmann, Y. Kutuvantavida, C. Kieninger, P.-I. Dietrich, M. Lauermann, S. Wolf, U. Troppenz, M. Moehrle, F. Merget, S. Skacel, J. Witzens, S. Randel, W. Freude, C. Koos, *Light Sci. Appl.* **2020**, *9*, 71.  
 [15] J. K. Hohmann, M. Renner, E. H. Waller, G. von Freymann, *Adv. Opt. Mater.* **2015**, *3*, 1488.  
 [16] C. Barner-Kowollik, M. Bastmeyer, E. Blasco, G. Delaittre, P. Müller, B. Richter, M. Wegener, *Angewandte Chem.* **2017**, *56*, 15828.  
 [17] E. Skliutas, M. Lebedevaitė, E. Kabouraki, T. Baldacchini, J. Ostrauskaite, M. Vamvakaki, M. Farsari, S. Juodkazis, M. Malinauskas, *Nanophotonics* **2021**, *10*, 1211.  
 [18] S. Varapnickas, M. Malinauskas, *Processes of Laser Direct Writing 3D Nanolithography, volume Handbook of Laser Micro- and Nano-Engineering*, Springer International Publishing, New York **2020**.  
 [19] A. Bertocini, S. P. Laptinok, L. Genchi, V. P. Rajamanickam, C. Liberale, *J. Biophotonics* **2021**, *14*, 1.  
 [20] S. Varapnickas, S.-C. Thodika, F. Morote, S. Juodkazis, M. Malinauskas, E. Brasselet, *Appl. Phys. Lett.* **2021**, *118*, 151104.  
 [21] M. Schmid, F. Sterl, S. Thiele, A. Herkommer, H. Giessen, *Opt. Lett.* **2021**, *3*, 2485.  
 [22] M. Schmid, D. Ludescher, H. Giessen, *Opt. Mater. Express* **2019**, *9*, 4564.  
 [23] M. Malinauskas, A. Žukauskas, V. Purlys, A. Gaidukevičiūtė, Z. Balevičius, A. Piskarskas, C. Fotakis, S. Pissadakis, D. Gray, R. Gadonas, M. Vamvakaki, M. Farsari, *Opt Lasers Eng* **2012**, *50*, 1785.  
 [24] X. Wen, B. Zhang, W. Wang, F. Ye, S. Yue, H. Guo, G. Gao, Y. Zhao, Q. Fang, C. Nguyen, X. Zhang, J. Bao, J. Robinson, P. Ajayan, J. Lou, *Nat. Mater.* **2021**, *20*, 1506.  
 [25] D. Gonzalez-Hernandez, S. Varapnickas, G. Merkininkaitė, A. Čiburys, D. Gailevičius, S. Šakirzanovas, S. Juodkazis, M. Malinauskas, *Photonics* **2021**, *8*, 1.  
 [26] D. Wu, S. Z. Wu, L. G. Niu, Q. D. Chen, R. Wang, J. F. Song, H. H. Fang, H. B. Sun, *Appl. Phys. Lett.* **2010**, *97*, 3.  
 [27] J. H. Atwater, P. Spinelli, E. Kosten, J. Parsons, C. Van Lare, J. Van De Groep, J. Garcia De Abajo, A. Polman, H. A. Atwater, *Appl. Phys. Lett.* **2011**, *99*, 3.  
 [28] S. Thiele, K. Arzenbacher, T. Gissibl, H. Giessen, A. Herkommer, *Sci. Adv.* **2017**, *3*, e1602655.  
 [29] B. Sanchez-Padilla, A. Žukauskas, A. Aleksanyan, A. Balčytis, M. Malinauskas, S. Juodkazis, E. Brasselet, *Opt. Express* **2016**, *24*, 24075.  
 [30] A. Bertocini, V. P. Rajamanickam, C. Liberale, in *2017 Conf. on Lasers and Electro-Optics Europe & European Quantum Electronics Conf. (CLEO/Europe-EQEC)*, IEEE, Munich **2017**, pp. 1–1.



- [31] S. Sivankutty, A. Bertocini, V. Tsvirkun, N. Gajendra Kumar, G. Brévalle, G. Bouwmans, E. R. Andresen, C. Liberale, H. Rigneault, *Opt. Lett.* **2021**, *46*, 4968.
- [32] C. Barner-Kowollik, M. Bastmeyer, E. Blasco, G. Delaittre, P. Muller, B. Richter, M. Wegener, *Ang. Chem.* **2017**, *56*, 15828.
- [33] M. Malinauskas, A. Žukauskas, S. Hasegawa, Y. Hayasaki, V. Mizeikis, R. Buivydas, S. Juodkazis, *Light Sci. Appl.* **2016**, *5*, e16133.
- [34] M. Malinauskas, P. Danilevicius, S. Juodkazis, *Opt. Express* **2011**, *19*, 5602.
- [35] D. Perevoznic, R. Nazir, R. Kiyam, K. Kurselis, B. Koszarna, D. T. Gryko, B. N. Chichkov, *Opt. Express* **2019**, *27*, 25119.
- [36] M. Thiel, J. Fischer, G. von Freymann, M. Wegener, *Appl. Phys. Lett.* **2010**, *97*, 221102.
- [37] D. Nguyen, Q. Tong, I. Ledoux-Rak, N. Lai, *J. Appl. Phys.* **2016**, *119*, 013101.
- [38] M. Malinauskas, A. Žukauskas, G. Bickaškaite, R. Gadonas, S. Juodkazis, *Opt. Express* **2010**, *18*.
- [39] P. Mueller, M. Thiel, M. Wegener, *Opt. Lett.* **2014**, *39*, 6847.
- [40] V. Hahn, T. Messer, N. M. Bojanowski, E. R. Curticean, I. Wacker, R. R. Schroder, E. Blasco, M. Wegener, *Nat. Photon.* **2021**, *15*, 932.
- [41] T. Tanaka, H.-B. Sun, S. Kawata, *Appl. Phys. Lett.* **2002**, *80*, 312.
- [42] J. Serbin, A. Ovsianikov, B. Chichkov, *Opt. Express* **2004**, *12*, 5221.
- [43] L. Jonusauskas, D. Gailevicius, S. Rekštyte, T. Baldacchini, S. Juodkazis, M. Malinauskas, *Opt. Express* **2019**, *27*, 15205.
- [44] T. Kondo, S. Juodkazis, V. Mizeikis, H. Misawa, S. Matsuo, *Opt. Express* **2006**, *14*, 7943.
- [45] E. Stankevicius, T. Gertus, M. Rutkauskas, M. Gedvilas, G. Raciukaitis, R. Gadonas, V. Smilgevičius, M. Malinauskas, *J. Micromech. Microeng.* **2012**, *22*, 065022.
- [46] M. Manousidaki, D. Papazoglou, M. Farsari, S. Tzortzakakis, *Opt. Lett.* **2020**, *45*, 85.
- [47] L. Yang, A. El-Tamer, U. Hinze, J. Li, Y. Hu, W. Huang, J. Chu, B. Chichkov, *Opt. Las. Eng.* **2015**, *70*, 26.
- [48] T. Zandrini, O. Shan, V. Parodi, C. G. M. Raimondi, R. Osellame, *Sci. Rep.* **2019**, *9*, 11761.
- [49] C. Maibohm, O. F. S. J. Borme, M. Sinou, K. Heggarty, J. B. Nieder, *Sci. Rep.* **2020**, *10*, 5506.
- [50] V. Hahn, P. Kiefer, T. Frenzel, J. Qu, E. Blasco, C. Barner-Kowollik, M. Wegener, *Adv. Func. Mater.* **2020**, *30*.
- [51] D. Loterie, P. Delrot, C. Moser, *Nat. Commun.* **2020**, *11*, 852.
- [52] P. Somers, Z. Liang, J. Johnson, B. Boudouris, L. Pan, X. Xu, *Light Sci. Appl.* **2021**, *10*, 199.
- [53] T. Buckmann, N. Stenger, M. Kadic, J. Kaschke, A. Frolich, T. Kennerknecht, C. Eberl, M. Thiel, M. Wegener, *Adv. Mater.* **2012**, *24*, 2710.
- [54] A. Žukauskas, M. Malinauskas, C. Reinhardt, B. N. Chichkov, R. Gadonas, *Appl. Opt.* **2012**, *51*, 4995.
- [55] D. Schäffner, T. Preuschoff, S. Ristok, L. Brozio, M. Schlosser, H. Giessen, G. Birkel, *Opt. Express* **2020**, *28*, 8640.
- [56] V. Pavelyev, V. Osipov, D. Kachalov, S. Khonina, W. Cheng, A. Gaidukeviciute, B. Chichkov, *Appl. Opt.* **2012**, *51*, 4215.
- [57] S. Ristok, S. Thiele, A. Toulouse, A. M. Herkommer, H. Giessen, *Opt. Mater. Express* **2020**, *10*, 2370.
- [58] D. Wu, Q. D. Chen, L. G. Niu, J. Jiao, H. Xia, J. F. Song, H. B. Sun, *IEEE Photon. Technol. Lett.* **2009**, *21*, 1535.
- [59] A. Landowski, D. Zepp, S. Wingerter, G. von Freymann, A. Widera, *APL Photonics* **2017**, *2*, 106102.
- [60] T. Aderneuer, O. Fernández, R. Ferrini, *Opt. Exp.* **2021**, *29*, 39511.
- [61] C. Ocier, C. A. Richards, D. A. Bacon-Brown, Q. Ding, R. Kumar, T. J. Garcia, J. van de Groep, J. H. Song, A. J. Cyphersmith, A. Rhode, A. N. Perry, A. J. Littlefield, J. Zhu, D. Xie, H. Gao, J. F. Messinger, M. L. Brongersma, K. C. Toussaint, L. L. Goddard, P. V. Braun, *Light Sci. Appl.* **2020**, *9*, 196.
- [62] X. Porte, N. U. Dinc, J. Moughames, G. Panusa, C. Juliano, K. Muamer, C. Moser, D. Brunner, D. Psaltis, *Optica* **2021**, *8*, 2.
- [63] F. Jin, J. Liu, Y.-Y. Zhao, X.-Z. Dong, M.-L. Zheng, X.-M. Duan, *Nat. Commun.* **2022**, *13*, 1357.
- [64] J. J. Xu, W. G. Yao, Z. N. Tian, L. Wang, K. M. Guan, Y. Xu, Q. D. Chen, J. A. Duan, H. B. Sun, *IEEE Photon. Technol. Lett.* **2015**, *27*, 2465.
- [65] X. F. Lin, Q. D. Chen, L. G. Niu, T. Jiang, W. Q. Wang, H. B. Sun, *J. Light. Technol.* **2010**, *28*, 1256.
- [66] S. Thiele, T. Gissibl, H. Giessen, A. M. Herkommer, *Opt. Lett.* **2016**, *41*, 3029.
- [67] T. Jiang, Q.-D. Chen, J. Zhang, Z.-N. Tian, L.-G. Niu, Q.-S. Li, H.-Y. Wang, L. Qin, H.-B. Sun, *Opt. Lett.* **2013**, *38*, 3739.
- [68] Z.-N. Tian, L.-J. Wang, Q.-D. Chen, T. Jiang, L. Qin, L.-J. Wang, H.-B. Sun, *Opt. Lett.* **2013**, *38*, 5414.
- [69] E. Johlin, S. A. Mann, S. Kasture, A. F. Koenderink, E. C. Garnett, *Nat. Commun.* **2018**, *9*, 4742.
- [70] T. T. Chung, Y. T. Tu, Y. H. Hsueh, S. Y. Chen, W. J. Li, *Int. J. Autom. Smart Technol.* **2013**, *3*, 131.
- [71] Z.-N. Tian, W.-G. Yao, J.-J. Xu, Y.-H. Yu, Q.-D. Chen, H.-B. Sun, *Opt. Lett.* **2015**, *40*, 4222.
- [72] P.-I. Dietrich, R. J. Harris, M. Blaicher, M. K. Corrigan, T. J. Morris, W. Freude, A. Quirrenbach, C. Koos, *Opt. Express* **2017**, *25*, 18288.
- [73] P. I. Dietrich, M. Blaicher, I. Reuter, M. Billah, T. Hoose, A. Hofmann, C. Caer, R. Dangel, B. Offrein, U. Troppenz, M. Moehrl, W. Freude, C. Koos, *Nat. Photonics* **2018**, *12*, 241.
- [74] H. Gehring, A. Eich, C. Schuck, W. H. P. Pernice, *Opt. Lett.* **2019**, *44*, 5089.
- [75] M. Trappen, M. Blaicher, P. I. Dietrich, C. Dankwart, Y. Xu, T. Hoose, M. R. Billah, A. Abbasi, R. Baets, U. Troppenz, M. Theurer, K. Wörhoff, M. Seyfried, W. Freude, C. Koos, *Opt. Express* **2020**, *28*, 37996.
- [76] K. R. Safronov, V. O. Bessonov, D. V. Akhremenkov, M. A. Sirotin, M. N. Romodina, E. V. Lyubin, I. V. Soboleva, A. A. Fedyanin, *Laser Photonics Rev.* **2022**, *2100542*, 2100542.
- [77] C. Liberale, G. Cojoc, F. Bragheri, P. Minzioni, G. Perozziello, R. La Rocca, L. Ferrara, V. Rajamanickam, E. Di Fabrizio, I. Cristiani, *Sci. Rep.* **2013**, *3*, 1258.
- [78] S. Bianchi, V. P. Rajamanickam, L. Ferrara, E. Di Fabrizio, C. Liberale, R. Di Leonardo, *Opt. Lett.* **2013**, *38*, 4935.
- [79] S. Yu, J. Lu, V. Ginis, S. Kheifets, S. W. D. Lim, M. Qiu, T. Gu, J. Hu, F. Capasso, *Optica* **2021**, *8*, 409.
- [80] M. Sartison, K. Weber, S. Thiele, L. Bremer, S. Fischbach, T. Herzog, S. Kolatschek, M. Jetter, S. Reitzenstein, A. Herkommer, P. Michler, S. L. Portalupi, H. Giessen, *Light Adv. Manuf.* **2021**, *2*, 6.
- [81] X. Cao, Y. Du, A. Küffner, J. Van Wyk, P. Arosio, J. Wang, P. Fischer, S. Stavrakis, A. DeMello, *Small* **2020**, *16*, 1.
- [82] Z. Xie, S. Feng, P. Wang, L. Zhang, X. Ren, L. Cui, T. Zhai, J. Chen, Y. Wang, X. Wang, W. Sun, J. Ye, P. Han, P. J. Klar, Y. Zhang, *Adv. Opt. Mater.* **2015**, *3*, 1232.
- [83] A. Bertocini, G. Cojoc, J. Guck, C. Liberale, *SPIE Proc.* **2020**, *1129211*, 36.
- [84] J. Williams, J. Smith, J. S. Suelzer, N. G. Usechak, H. Chandralim, in *Proceedings of IEEE Sensors*, IEEE, Piscataway, NJ **2020**, pp. 1–4.
- [85] H. Wang, H. Wang, W. Zhang, K. Yang, *ACS Nano* **2020**, *14*, 10452.
- [86] B. Jia, J. Serbin, H. Kim, B. Lee, J. Li, M. Gu, *Appl. Phys. Lett.* **2007**, *90*, 7.
- [87] Q. D. Chen, D. Wu, L. G. Niu, J. Wang, X. F. Lin, H. Xia, H. B. Sun, *Appl. Phys. Lett.* **2007**, *91*, 1.
- [88] D. Wu, L.-G. Niu, Q.-D. Chen, R. Wang, H.-B. Sun, *Opt. Lett.* **2008**, *33*, 2913.
- [89] Q.-D. Chen, X.-F. Lin, L.-G. Niu, D. Wu, W.-Q. Wang, H.-B. Sun, *Opt. Lett.* **2008**, *33*, 2559.
- [90] V. Pavelyev, V. Osipov, D. Kachalov, B. Chichkov, *Opt. Commun.* **2013**, *286*, 368.

- [91] U. T. Sanli, H. Ceylan, I. Bykova, M. Weigand, M. Sitti, G. Schütz, K. Keskinbora, *Adv. Mater.* **2018**, *30*, 1802503.
- [92] W. Hadibrata, H. Wei, S. Krishnaswamy, K. Aydin, *Nano Lett.* **2021**, *21*, 2422.
- [93] S. Thiele, C. Pruss, A. M. Herkommer, H. Giessen, *Opt. Express* **2019**, *27*, 35621.
- [94] L. Yan, D. Yang, Q. Gong, Y. Li, *Micromachines* **2020**, *11*, 112.
- [95] V. Hahn, S. Kalt, G. M. Sridharan, M. Wegener, S. Bhattacharya, *Opt. Express* **2018**, *26*, 33148.
- [96] H. Wei, F. Callewaert, W. Hadibrata, V. Velev, Z. Liu, P. Kumar, K. Aydin, S. Krishnaswamy, *Adv. Opt. Mater.* **2019**, *7*, 1900513.
- [97] S. Zanotto, F. Sgrignuoli, S. Nocentini, D. Martella, C. Parmeggiani, D. S. Wiersma, *Appl. Phys. Lett.* **2019**, *114*, 201103.
- [98] X. Wang, A. A. Kuchmizhak, E. Brasselet, S. Juodkazis, *Appl. Phys. Lett.* **2017**, *110*, 181101.
- [99] A. Bertocini, C. Liberale, *Optica* **2020**, *7*, 1487.
- [100] M. Schumann, T. Bückmann, N. Gruhler, M. Wegener, W. Pernice, *Light Sci. Appl.* **2014**, *3*, e175.
- [101] Z. Hou, X. Xiong, J. Cao, Q. Chen, Z. Tian, X. Ren, H. Sun, *Adv. Opt. Mater.* **2019**, *7*, 1900129.
- [102] A. Nestic, M. Blaicher, P. Marin-Palomo, C. Füllner, S. Randel, W. Freude, C. Koos, *arXiv* **2021**.
- [103] A. Bertocini, C. Liberale, *IEEE Photon. Technol. Lett.* **2018**, *30*, 1882.
- [104] K. Vanmol, T. Baghdasaryan, N. Vermeulen, K. Saurav, J. Watté, H. Thienpont, J. Van Erps, *Opt. Express* **2020**, *28*, 36147.
- [105] C. Jain, A. Braun, J. Gargiulo, B. Jang, G. Li, H. Lehmann, S. A. Maier, M. A. Schmidt, *ACS Photonics* **2019**, *6*, 649.
- [106] B. Jang, J. Gargiulo, J. Kim, J. Bürger, S. Both, H. Lehmann, T. Wieduwilt, T. Weiss, S. A. Maier, M. A. Schmidt, *APL Photonics* **2021**, *6*, 6.
- [107] C. Jörg, F. Letscher, M. Fleischhauer, G. von Freymann, *New J. Phys.* **2017**, *19*, 083003.
- [108] A. Žukauskas, I. Matulaitienė, D. Paipulas, G. Niaura, M. Malinauskas, R. Gadonas, *Laser Photonics Rev.* **2015**, *9*, 706.
- [109] S. Dottermusch, D. Busko, M. Langenhorst, U. W. Paetzold, B. S. Richards, *Opt. Lett.* **2019**, *44*, 29.
- [110] C. Jörg, G. Queraltó, M. Kremer, G. Pelegrí, J. Schulz, A. Szameit, G. von Freymann, J. Mompart, V. Ahufinger, *Light Sci. Appl.* **2020**, *9*, 150.
- [111] A. Grabulosa, J. Moughames, X. Porte, D. Brunner, *Nanophotonics* **2022**, *11*, 1591.
- [112] E. Brasselet, M. Malinauskas, A. Žukauskas, S. Juodkazis, *Appl. Phys. Lett.* **2010**, *97*, 211108.
- [113] K. Weber, F. Hütt, S. Thiele, T. Gissibl, A. Herkommer, H. Giessen, *Opt. Express* **2017**, *25*, 19672.
- [114] E. Stegenburgs, A. Bertocini, A. Trichili, M. S. Alias, T. K. Ng, M.-S. Alouini, C. Liberale, B. S. Ooi, *IEEE Commun. Mag.* **2019**, *57*, 65.
- [115] S. Schmidt, S. Thiele, A. Toulouse, C. Bösel, T. Tiess, A. Herkommer, H. Gross, H. Giessen, *Optica* **2020**, *7*, 1279.
- [116] J. M. Oliveira, A. J. Jesus-Silva, E. J. Fonseca, *Opt Laser Technol* **2019**, *119*, 105632.
- [117] A. Žukauskas, M. Malinauskas, E. Brasselet, *Appl. Phys. Lett.* **2013**, *103*, 181122.
- [118] Z.-N. Tian, X.-W. Cao, W.-G. Yao, P.-X. Li, Y.-H. Yu, G. Li, Q.-D. Chen, H.-B. Sun, *IEEE Photon. Technol. Lett.* **2016**, *28*, 2299.
- [119] A. Balčytis, D. Hakobyan, M. Gabalis, A. Žukauskas, D. Urbonas, M. Malinauskas, R. Petruškevičius, E. Brasselet, S. Juodkazis, *Opt. Express* **2016**, *24*, 16988.
- [120] V. S. Lyubopytov, A. P. Porfirev, S. O. Gurbatov, S. Paul, M. F. Schumann, J. Cesar, M. Malekizandi, M. T. Haidar, M. Wegener, A. Chipouline, F. Küppers, *Opt. Express* **2017**, *25*, 9634.
- [121] Z.-N. Tian, Q.-D. Chen, Z.-Y. Hu, Y.-K. Sun, Y.-H. Yu, H. Xia, H.-B. Sun, *Opt. Lett.* **2018**, *43*, 3116.
- [122] Z.-Y. Hu, Z.-N. Tian, J.-G. Hua, Q.-D. Chen, H.-B. Sun, *Appl. Phys. Lett.* **2020**, *117*, 021101.
- [123] Z. Xie, S. Gao, T. Lei, S. Feng, Y. Zhang, F. Li, J. Zhang, Z. Li, X. Yuan, *Photonics Research* **2018**, *6*, 743.
- [124] A. Žukauskas, V. Melissinaki, D. Kaškelyte, M. Farsari, M. Malinauskas, *J. Laser Micro Nanoeng.* **2014**, *9*, 68.
- [125] G. S. Sokolovskii, V. Melissinaki, K. A. Fedorova, V. V. Dudelev, S. N. Losev, V. E. Bougrov, W. Sibbett, M. Farsari, E. U. Rafailov, *Sci. Rep.* **2018**, *8*, 14618.
- [126] I. Reddy, A. Bertocini, C. Liberale, *Optica* **2022**, *9*, 645.
- [127] G. X. Jin, X. Y. Hu, Z. C. Ma, C. H. Li, Y. L. Zhang, H. B. Sun, *Nanotechnology and Precision Engineering* **2019**, *2*, 110.
- [128] T. Gissibl, S. Thiele, A. Herkommer, H. Giessen, *Nat. Photonics* **2016**, *10*, 554.
- [129] M. A. Tadayon, S. Chaitanya, K. M. Martyniuk, J. C. McGowan, S. P. Roberts, C. A. Denny, M. Lipson, *Opt. Express* **2019**, *27*, 22352.
- [130] B. Wang, Q. Zhang, M. Gu, *Opt. Mater. Express* **2020**, *10*, 3174.
- [131] A. Antonini, A. Sattin, M. Moroni, S. Bovetti, C. Moretti, F. Succol, A. Forli, D. Vecchia, V. P. Rajamanickam, A. Bertocini, S. Panzeri, C. Liberale, T. Fellin, *eLife* **2020**, *9*, e58882.
- [132] J. Li, P. Fejes, D. Lorensen, B. C. Quirk, P. B. Noble, R. W. Kirk, A. Orth, F. M. Wood, B. C. Gibson, D. D. Sampson, R. A. McLaughlin, *Sci. Rep.* **2018**, *8*, 14789.
- [133] J. Li, S. Thiele, B. C. Quirk, R. W. Kirk, J. W. Verjans, E. Akers, C. A. Bursill, S. J. Nicholls, A. M. Herkommer, H. Giessen, R. A. McLaughlin, *Light Sci. Appl.* **2020**, *9*, 124.
- [134] J. Li, S. Thiele, R. W. Kirk, B. C. Quirk, A. Hoogendoorn, Y. C. Chen, K. Peter, S. J. Nicholls, J. W. Verjans, P. J. Psaltis, C. Bursill, A. M. Herkommer, H. Giessen, R. A. McLaughlin, *Small* **2022**, *21*, 2107032.
- [135] K. Yanny, N. Antipa, W. Liberti, S. Dehaeck, K. Monakhova, F. L. Liu, K. Shen, R. Ng, L. Waller, *Light Sci. Appl.* **2020**, *9*, 171.
- [136] V. Melissinaki, O. Tsilipakos, M. Kafesaki, M. Farsari, S. Pissadakis, *IEEE J. Sel. Top. Quantum Electron.* **2021**, *27*, 59.
- [137] A. Asadollahbaik, S. Thiele, K. Weber, A. Kumar, J. Drozella, F. Sterl, A. M. Herkommer, H. Giessen, J. Fick, *ACS Photonics* **2020**, *7*, 88.
- [138] A. Toulouse, S. Thiele, H. Giessen, A. M. Herkommer, *Opt. Lett.* **2018**, *43*, 5283.
- [139] K. Weber, Z. Wang, S. Thiele, A. Herkommer, H. Giessen, *Opt. Lett.* **2020**, *45*, 2784.
- [140] A. Toulouse, J. Drozella, S. Thiele, H. Giessen, A. Herkommer, *Light: Advanced Manufacturing* **2021**, *2*, 20.
- [141] A. Toulouse, J. Drozella, P. Motzfeld, N. Fahrbach, V. Aslani, S. Thiele, H. Giessen, A. M. Herkommer, *Opt. Express* **2022**, *30*, 707.
- [142] A. Ashkin, *Phys. Rev. Lett.* **1970**, *24*, 156.
- [143] M. Plidschun, H. Ren, J. Kim, R. Förster, S. A. Maier, M. A. Schmidt, *Light Sci. Appl.* **2021**, *10*, 57.
- [144] A. Kumar, A. Asadollahbaik, J. Kim, K. Lahlil, S. Thiele, A. M. Herkommer, S. N. Chormaic, J. Kim, T. Gacoin, H. Giessen, J. Fick, *Photonics Research* **2022**, *10*, 332.
- [145] A. Asadollahbaik, A. Kumar, M. Heymann, H. Giessen, J. Fick, *Opt. Lett.* **2022**, *47*, 170.
- [146] V. Melissinaki, M. Vamvakaki, M. Farsari, S. Pissadakis, in *2013 Conf. on Lasers & Electro-Optics Europe & Int. Quantum Electronics Conf. CLEO EUROPE/IQEC*, IEEE, Piscataway, NJ **2013**, pp. 1–1.
- [147] V. Melissinaki, I. Konidakis, M. Farsari, S. Pissadakis, *IEEE Sens. J.* **2016**, *16*, 7094.
- [148] J. W. Smith, J. C. Williams, J. S. Suelzer, N. G. Usechak, H. Chandralhim, *J. Micromech. Microeng.* **2020**, *30*, 125007.
- [149] H. E. Williams, D. J. Freppon, S. M. Kuebler, R. C. Rumpf, M. A. Melino, *Opt. Express* **2011**, *19*, 22910.
- [150] M. Goraus, I. Martincek, P. Urbancova, D. Pudis, D. Kacik, in *Proc. ELEKTRO 2020*, IEEE, Taormina, Italy **2020**, pp. 1–4.

- [151] S. Rekstyte, D. Paipulas, V. Mizeikis, *Opt. Lett.* **2019**, *44*, 4602.
- [152] S. Zhang, S. Tang, S. Feng, Y. Xiao, W. Cui, X. Wang, W. Sun, J. Ye, P. Han, X. Zhang, Y. Zhang, *Adv. Opt. Mater.* **2019**, *7*, 1900602.
- [153] Q. Liu, Y. Zhan, S. Zhang, S. Feng, X. Wang, W. Sun, J. Ye, Y. Zhang, *Opt. Express* **2020**, *28*, 11730.
- [154] D. Zhang, H. Wei, S. Krishnaswamy, *IEEE Photon. Technol. Lett.* **2019**, *31*, 1725.
- [155] M. Power, A. J. Thompson, S. Anastasova, G.-Z. Yang, *Small* **2018**, *14*, 1703964.
- [156] R. Förster, S. Weidlich, M. Nissen, T. Wieduwilt, J. Kobelke, A. M. Goldfain, T. K. Chiang, R. F. Garmann, V. N. Manoharan, Y. Lahini, M. A. Schmidt, *ACS Sensors* **2020**, *5*, 879.
- [157] P. Dietrich, G. Göring, M. Trappen, M. Blaicher, W. Freude, T. Schimmel, H. Hölscher, C. Koos, *Small* **2019**, *16*, 1904695.
- [158] M. Zou, C. Liao, S. Liu, C. Xiong, C. Zhao, J. Zhao, Z. Gan, Y. Chen, K. Yang, D. Liu, Y. Wang, Y. Wang, *Light Sci. Appl.* **2021**, *10*, 171.
- [159] S. Klein, A. Barsella, H. Leblond, H. Bulou, A. Fort, C. Andraud, G. Lemerrier, J. C. Mulatier, K. Dorkenoo, *Appl. Phys. Lett.* **2005**, *86*, 211118.
- [160] N. Lindenmann, G. Balthasar, D. Hillerkuss, R. Schmogrow, M. Jordan, J. Leuthold, W. Freude, C. Koos, *Opt. Express* **2012**, *20*, 17667.
- [161] N. Lindenmann, S. Dottermusch, M. L. Goedecke, T. Hoose, M. R. Billah, T. P. Onanuga, A. Hofmann, W. Freude, C. Koos, *J. Light. Technol.* **2014**, *33*, 755.
- [162] M. R. Billah, M. Blaicher, T. Hoose, P.-I. Dietrich, P. Marin-Palomo, N. Lindenmann, A. Nestic, A. Hofmann, U. Troppenz, M. Moehle, S. Randel, W. Freude, C. Koos, *Optica* **2018**, *5*, 876.
- [163] C.-W. Lee, S. Pagliara, U. Keyser, J. J. Baumberg, *Appl. Phys. Lett.* **2012**, *100*, 171102.
- [164] A. Nestic, M. Blaicher, T. Hoose, A. Hofmann, M. Laueremann, Y. Kutuvantavida, M. Nöllenburg, S. Randel, W. Freude, C. Koos, *Opt. Express* **2019**, *27*, 17402.
- [165] S. Nocentini, F. Riboli, M. Burresi, D. Martella, C. Parmeggiani, D. S. Wiersma, *ACS Photonics* **2018**, *5*, 3222.
- [166] H. Gehring, M. Blaicher, W. Hartmann, P. Varytis, K. Busch, M. Wegener, W. H. P. Pernice, *APL Photonics* **2019**, *4*, 010801.
- [167] K. Vanmol, S. Tuccio, V. Panapakkam, H. Thienpont, J. Watte, J. Van Erps, *Opt Laser Technol* **2019**, *112*, 292.
- [168] P. Nair, J. Trisno, H. Wang, J. Yang, *Int. J. Extrem. Manuf.* **2021**, *3*, 015301.
- [169] A. W. Schell, J. Kaschke, J. Fischer, R. Henze, J. Wolters, M. Wegener, O. Benson, *Sci. Rep.* **2013**, *3*, 1577.
- [170] S. Fischbach, A. Schlehahn, A. Thoma, N. Srocka, T. Gissibl, S. Ristok, S. Thiele, A. Kaganskiy, A. Strittmatter, T. Heindel, S. Rodt, A. Herkommer, H. Giessen, S. Reitzenstein, *ACS Photonics* **2017**, *4*, 1327.
- [171] L. Bremer, K. Weber, S. Fischbach, S. Thiele, M. Schmidt, A. Kaganskiy, S. Rodt, A. Herkommer, M. Sartison, S. L. Portalupi, P. Michler, H. Giessen, S. Reitzenstein, *APL Photonics* **2020**, *5*, 106101.
- [172] A. Landowski, J. Gutsche, S. Guckenbiehl, M. Schönberg, G. Von Freymann, A. Widera, *APL Photonics* **2020**, *5*, 016101.
- [173] A. Eich, T. C. Spiekermann, H. Gehring, L. Sommer, J. R. Bankwitz, P. P. J. Schrinner, J. A. Preuß, S. Michaelis de Vasconcellos, R. Bratschitsch, W. H. P. Pernice, C. Schuck, *ACS Photonics* **2022**, *9*, 551.
- [174] F. Davidson-Marquis, J. Gargiulo, E. Gómez-López, B. Jang, T. Kroh, C. Müller, M. Ziegler, S. A. Maier, H. Kübler, M. A. Schmidt, O. Benson, *Light Sci. Appl.* **2021**, *10*, 114.
- [175] E. Goi, M. Gu, *Proc. 2019 Conf. on Lasers and Electro-Optics Europe (CLEO Europe)*, OSA Technical Digest, Munich, Germany **2019**, Part F143-, 41566.
- [176] H. Ren, W. Shao, Y. Li, F. Salim, M. Gu, *Sci. Adv.* **2020**, *6*, eaaz4261.
- [177] E. Goi, X. Chen, Q. Zhang, B. P. Cumming, S. Schoenhardt, H. Luan, M. Gu, *Light Sci. Appl.* **2021**, *10*, 40.
- [178] E. Goi, S. Schoenhardt, M. Gu, in *2021 Conf. on Lasers and Electro-Optics (CLEO)*, San Jose, CA, OSA Technical Digest, **2021**, paper AW4D.3.
- [179] J. Moughames, X. Porte, M. Thiel, G. Ulliac, L. Larger, M. Jacquot, M. Kadic, D. Brunner, *Optica* **2020**, *7*, 640.
- [180] G. Panusa, N. U. Dinc, D. Psaltis, *Opt. Express* **2022**, *30*, 2564.
- [181] X. Lee, S. Saha, S. Sarkar, B. Giera, *Add. Manuf.* **2020**, *36*, 101444.
- [182] M. Malinauskas, H. Gilbergs, A. Žukauskas, V. Purlys, D. Paipulas, R. Gadonas, *J. Opt.* **2010**, *12*, 035204.
- [183] M. Schmid, D. Ludescher, H. Giessen, *Opt. Mater. Express* **2019**, *9*, 4564.
- [184] A. Žukauskas, M. Malinauskas, L. Kontenis, V. Purlys, D. Paipulas, G. Vengris, R. Gadonas, *Lith. J. Phys.* **2010**, *50*, 55.
- [185] P. Prabhakaran, K.-K. Jang, Y. Son, D.-Y. Yang, K.-S. Lee, *Mol. Cryst. Liq. Cryst.* **2013**, *578*, 4.
- [186] Q. Hu, X.-Z. Sun, C. Parmenter, M. Fay, E. Smith, G. Rance, Y. He, F. Zhang, Y. Liu, D. Irvine, C. Tuck, R. Hague, R. Wildman, *Sci. Rep.* **2017**, *7*, 17150.
- [187] J. Winczewski, M. Herrera, C. Cabriel, I. Izeddin, S. Gabel, B. Merle, A. S. Arce, H. Gardeniers, *Adv. Opt. Mater.* **2022**, 2102758.
- [188] N. Vasilantonakis, K. Terzaki, I. Sakellari, V. Purlys, D. Gray, C. Soukoulis, M. Vamvakaki, M. Kafesaki, M. Farsari, *Adv. Mater.* **2012**, *24*, 1101.
- [189] S. Puce, E. Sciurti, F. Rizzi, B. Spagnolo, A. Qualtieri, M. D. Vittorio, U. Stauer, *Micro Nano Eng.* **2019**, *2*, 70.
- [190] S. Ristok, P. Flad, H. Giessen, *Opt. Mater. Express* **2022**, *12*, 2063.
- [191] M. Sharipova, T. Baluyan, K. Abrashitova, G. Kulagin, A. Petrov, A. Chizhov, T. Shatalova, D. Chubich, D. Kolymagin, A. Vitukhnovsky, V. Bessonov, A. A. Fedyanin, *Opt. Mater. Express* **2021**, *11*, 371.
- [192] D. Gailevicius, V. Padolskyte, L. Mikoliunaite, S. Sakirzanovas, S. Juodkazis, M. Malinauskas, *Nanoscale Horiz.* **2019**, *4*, 647.
- [193] F. Kotz, A. S. Quick, P. Risch, T. Martin, T. Hoose, M. Thiel, D. Helmer, B. E. Rapp, *Adv. Mater.* **2021**, *33*, 2006341.
- [194] G. Merkininkaite, E. Aleksandravicius, M. Malinauskas, D. Gailevicius, S. Sakirzanovas, *Opto-Electron. Adv.* **2022**, *5*, 210077.
- [195] I. Cooperstein, S. C. Indukuri, A. Bouketov, U. Levy, S. Magdassi, *Adv. Mater.* **2020**, *32*, 2001675.
- [196] N. Chidambaram, R. Kirchner, R. Fallica, L. Yu, M. Altana, H. Schiff, *Adv. Mater. Technol.* **2017**, *2*, 1700018.
- [197] E. Balciunas, L. Jonusauskas, V. Valuckas, D. Baltrukiene, V. Bukelskiene, R. Gadonas, M. Malinauskas, *Proc. SPIE* **2012**, *8427*, 84271X.
- [198] J. Bauer, A.-G. Izard, Y. Zhang, T. Baldacchini, L. Valdevit, *Opt. Express* **2020**, *28*, 20362.
- [199] A. Žukauskas, G. Bataviciute, M. Sciuka, T. Jukna, A. Melninkaitis, M. Malinauskas, *Opt. Mater. Express* **2014**, *4*, 1601.
- [200] A. Žukauskas, G. Bataviciute, M. Sciuka, Z. Balevicius, A. Melninkaitis, M. Malinauskas, *Opt. Mater.* **2015**, *39*, 224.
- [201] L. Jonušauskas, D. Gailevičius, L. Mikoliūnaitė, D. Sakalauskas, S. Šakirzanovas, S. Juodkazis, M. Malinauskas, *Materials* **2017**, *10*, 12.
- [202] A. Butkute, L. Čekanavicius, G. Rimselis, D. Gailevicius, V. Mizeikis, A. Melninkaitis, T. Baldacchini, L. Jonusauskas, M. Malinauskas, *Opt. Lett.* **2020**, *45*, 13.
- [203] E. Kabouraki, V. Melissinaki, A. Yadav, A. Melninkaitis, K. Tourlouki, T. Tachtsidis, N. Kehagias, G. Barmparis, D. Papazoglou, E. Rafailov, M. Farsari, *Nanophotonics* **2021**, *10*, 3759.
- [204] M. Farsari, A. Ovsianikov, M. Vamvakaki, I. Sakellari, D. Gray, B. N. Chichkov, C. Fotakis, *Appl. Phys. A* **2008**, *93*, 11.
- [205] Y.-L. Sun, W.-F. Dong, L.-G. Niu, T. Jiang, D.-X. Liu, L. Zhang, Y.-S. Wang, Q.-D. Chen, D.-P. Kim, H.-B. Sun, *Light Sci. Appl.* **2014**, *3*, e129.
- [206] Z. Bayindir, Y. Sun, M. J. Naughton, *Appl. Phys. Lett.* **2005**, *86*, 064.
- [207] Q. Hu, G. A. Rance, G. F. Trindade, D. Pervan, L. Jiang, A. Foerster, L. Turyanska, C. Tuck, D. J. Irvine, R. Hague, R. D. Wildman, *Addit. Manuf.* **2022**, *51*, 102575.





**Diana Gonzalez-Hernandez** is a Ph.D. student in the Vibrational Imaging (VIBRA) Lab under the supervision of Prof. Carlo Liberale. She has been awarded the Al-Khwarizmi Fellowship by KAUST (Saudi Arabia) to pursue her doctoral studies. She received her M.Sc. double degree in 2021 with the Europhotonics International Scholarship in Physics from Aix-Marseille Université (France), and Technological Science from Vilnius University (Lithuania). Currently, she continues her research focused on the design of novel micro-optical systems fabricated via high-resolution two-photon lithography 3D printing.



**Andrea Bertoncini** is a process engineer at Nanoscribe GmbH & Co. KG (Germany), which is a pioneering company in the field of high-precision additive manufacturing based on multi-photon lithography. He defended his Ph.D. in 2020 at KAUST (Saudi Arabia), under the supervision of Carlo Liberale. His current work focuses on the development of grayscale two-photon lithography for the development of 3D-printed micro-optical elements.



**Carlo Liberale** is heading the Vibrational Imaging (VIBRA) Lab at KAUST (Saudi Arabia). His research interests are focused on developing and applying label-free chemical imaging based on vibrational spectroscopy. He is also interested in using high-resolution 3D printing based on two-photon lithography to fabricate novel micro-optics toward the miniaturization of complex optical systems for beam shaping, optical tweezers, and micro-endoscopy.



**Mangirdas Malinauskas** defended Ph.D. in 2010 at Vilnius University, Laser Research Center—“Laser Fabrication of Functional 3D Polymeric Micro/Nanostructures,” supervisor Prof. R. Gadonas. During his career, he has made traineeships in LZH (Prof. B.N. Chichkov) and IESL-FORTH (Dr. M. Farsari). In 2019–2022, he was a specially appointed Professor at Tokyo Institute of Technology (Tokyo, Japan), group of Prof. J. Morikawa. Currently, he continues investigation and fundamental study of laser 3D micro-/nano-structuring of cross-linkable materials for applications in microoptics, nanooptics (photonics), and biomedicine at VU LRC. Financing for the laboratory is acquired via national, European, and worldwide (NATO, US Army) funding schemes.